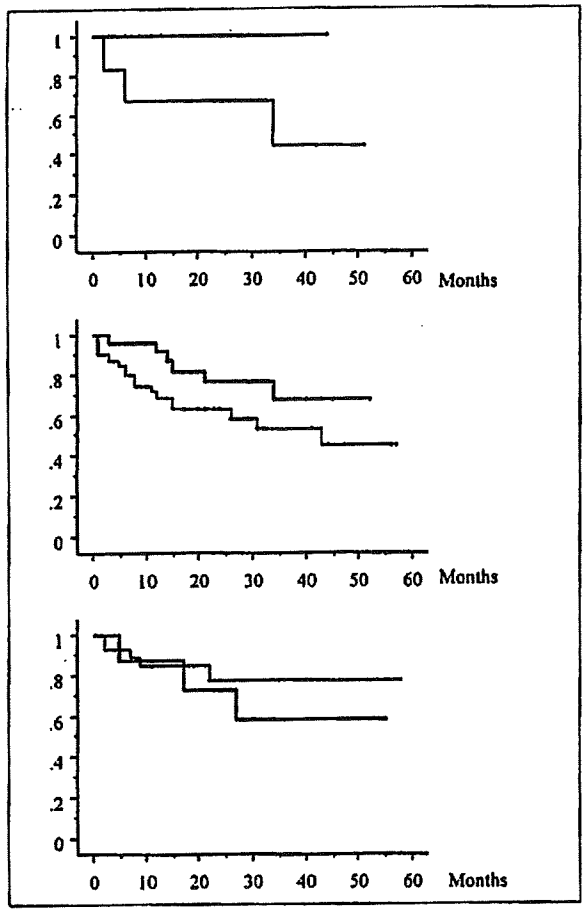


**FIGURE 3**
Cumulative overall survival curves with or without risk factors of metabolic syndrome.Upper panel: group B; middle panel: group C; and lower panel: group NBNC. The thin and bold lines denote patients with and without risk factors of metabolic syndrome, respectively. There were no significant differences among all groups, although groups B and C with risk factors for metabolic syndrome had a tendency toward lower survival rates than those without.

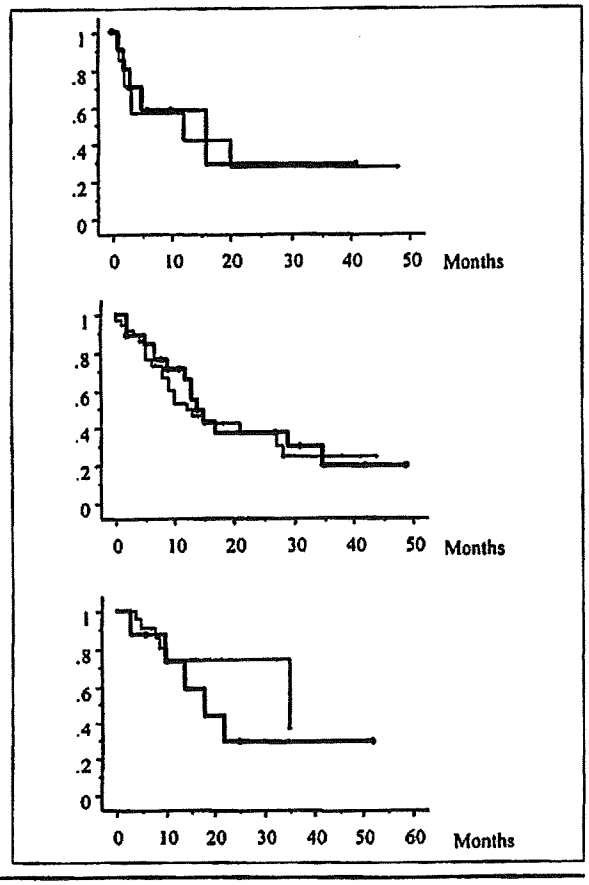


**FIGURE 4**
Disease-free survival curves with or without risk factors of metabolic syndrome.Upper panel: group B; middle panel: group C; and lower panel: group NBNC. The thin and bold lines denote patients with and without risk factors of metabolic syndrome, respectively. There were no significant differences among all groups.

with or without HBcAb (data not shown).

Seven out of the 37 patients from the NBNC group showed various degrees of fatty changes in their liver histology. Among them, 3 patients who did not have a history of alcohol abuse were strongly suspected to have NASH (8.1%). The clinical features of these 3 patients with HCC associated with NASH are shown in **Table 5**. We estimated both the necroinflammatory grade and the fibrosis score according to the definitions proposed by Brunt *et al.* (27). The BMIs of these three patients were 23.1, 24.8, and 24.4, respectively. These figures were within the normal range according to western standards but are considered to be overweight by Asian standards (28). Two of the 3 patients had associated diabetes mellitus, and 1 patient had no risk factors for MS.

## DISCUSSION

In this study, the background and associated conditions of patients with HCC who underwent surgery in relation to viral markers was investigated, and then compared to determine participation of risk factors for MS in the development of HCC, in particular non-B non-C HCC. At first, the prevalence of chronic hepatitis and liver cirrhosis in non-B non-C HCC was confirmed to be almost the same as in group B, and was significantly lower than in group C, although there were no differences in the preoperative Child-Pugh classifications among the 3 groups.

One of the current topics in this field is the relationship between obesity and HCC (15,18). In this study, the mean BMI was less than 25kg/m$^2$ in all 3 groups, and there were no significant differences among them. However, the NBNC group showed the highest ratio of patients with a BMI greater than 25kg/m$^2$, suggesting the possible participation of obesity in non-B non-C HCC.

This study also demonstrated that patients in NBNC group had a significantly higher prevalence of both diabetes mellitus and hyperlipidemia, and their mean serum TG was significantly higher than groups B and C. This result showed that non-B non-C HCC may be strongly associated with metabolic or insulin resistance syndrome, as suggested in other reports (16,20). Diabetes mellitus has been recognized as a risk factor of not only chronic liver disease, but also HCC (14-17). Bugianesi *et al.* (20) reported that the prevalence of diabetes and the plasma levels of both TC and TG were significantly higher in those patients with HCC associated with cryptogenic cirrhosis than in patients with alcohol and hepatitis virus infection related HCC. However, in this study, the prevalence of alcohol abuse was significantly higher in the NBNC group than in group C. Therefore, we performed an additional analysis after excluding those patients with alcohol abuse. Based on that analysis, no significant difference in the prevalence of diabetes mellitus and hyperlipidemia among the 3 groups was found, although the serum TG and TC levels were still higher. In contrast to these results, some studies have indicated that alco-

Table 5 Three cases of HCC associated with NASH

| | Case 1 | Case 2 | Case 3 |
|---|---|---|---|
| Age | 69 | 72 | 79 |
| Gender | Male | Female | Male |
| BMI (kg/m²) | 23.1 | 24.8 | 24.4 |
| Diabetes mellitus | - | + | + |
| Hypertension | - | + | - |
| Hyperlipidemia | - | + | + |
| AST (IU/L) | 23 | 59 | 59 |
| ALT (IU/L) | 23 | 46 | 76 |
| PLT (×10⁴/mm³) | 15.6 | 16 | 11.8 |
| Total Cholesterol (mg/dL) | 212 | 217 | 207 |
| Triglyceride (mg/dL) | 70 | 95 | 205 |
| Steatosis* | mild | moderate | moderate |
| Degeneration of hepatocyte* | mild | ballooning and acidophilic bodies | Mallory bodies and acidophilic bodies |
| Intraacinar inflammatory cells* | scattered microabscess | many microabscess | many microabscess |
| Portal inflammation* | mild | moderate to severe | moderate to severe |
| Necroinflammatory grade* | 1 | 2 | 3 |
| Fibrosis stage* | 3 | 4 | 4 |

*Definitions according to Brunt *et al.* (27)

hol intake was associated with a lower prevalence of MS (29,30). In the patients studied here, however, chronic liver disease, risk factors for MS, and alcohol abuse might all participate in the carcinogenesis of HCC in a very complex fashion.

More recently, NAFLD including NASH has been considered to be one of the causes of chronic liver disease (15,31) and HCC (19-25). Although the prevalence of NASH in HCC patients remains unknown, in the literature, HCC has been observed in 2.4-13% of NASH patients (21,23,24). Bugianesi *et al.* (20) reported that among 641 cirrhosis-associated HCCs, 44 patients (6.9%) had cryptogenic cirrhosis which was associated with NASH. On the other hand, Yano *et al.* (12) stated that there were no non-B non-C patients with HCC in whom NASH was thought to be the cause. However, it is difficult to clearly determine the participation of NASH in the pathogenesis of HCC associated with cryptogenic cirrhosis, because the steatosis might decrease or disappear when the NASH progressed to cirrhosis (17,18,20,23,31). In the present study, 3 patients were judged to be associated with NASH based on microscopic findings of moderate to severe macrovesicular steatosis, hepatocellular ballooning, lobular inflammation with necrosis of the hepatocytes, and perisinusoidal fibrosis. Although there was some discussion about the histopathological findings in NAFLD (19), macro-vesicular steatosis, Mallory's hyaline, ballooning, lobular inflammation, and perisinusoidal fibrosis were considered to be histological features in general (19,31,32).

In this study, the cumulative overall and disease free 3-year survival rates for HCC in the non-B non-C patients after surgery were 69.8% and 27.6%, respectively, and there were no significant differences in both the cumulative overall and disease free survival rates among the B, C, and NBNC patients. Although this study population contained 26 patients who had already underwent some treatment for HCC, these results were considered to be almost the same as with previous studies (8,10,11,33). HCC in the non-B non-C patients has been reported to have a worse prognosis than HCC due to other causes. With respect to the influence of the risk factors for MS on survival, the interesting result was obtained that these risk factors might exhibit an adverse effect on the survival of hepatitis virus related HCC patients, but not on non-B non-C HCC patients, although their survival rates did not show any statistically significant differences because of the small number of cases studied. One could speculate that the risk factors for MS had a positive impact on the occurrence of non-B non-C HCC, but may exert a negative impact on the prognosis of hepatitis virus related HCC patients.

In conclusion, the prevalence of diabetes mellitus, hyperlipidemia, and the plasma triglyceride level were all significantly higher in non-B non-C HCC patients as compared with those with HCC related to both HBV and HCV infection. This suggests that the pathogenesis of non-B non-C HCC was more closely associated with the risk factors for MS than viral related HCC. However, alcohol abuse affected the pathological mechanisms at least in part. With respect to the participation of NASH, 3 out of 37 non-B non-C HCC patients were clearly associated with NASH from the viewpoint of their clinical and histological analyses. The prognosis of patients with positive viral markers tended to be worse in those patients who also had risk factors for MS than those without. On the other hand, there was no such tendency in the non-B non-C patients. To our knowledge, this is the first report of its kind on HCC patients with and without hepatitis virus markers, and the findings presented here may be informative in a clinical setting.

## REFERENCES


1 Llovet JM, Burroughs A, Bruix J: Hepatocellular carcinoma. Lancet 2003; 362:1907-1917.
2 Ercolani G, Grazi GL, Ravaioli M, Del Gaudio M, Gardini A, Cescon M, Varotti G, Cetta F, Cavallari A: Liver resection for hepatocellular carcinoma on cirrhosis: univariate and multivariate analysis of risk factors for intrahepatic recurrence. Ann Surg 2003; 237:536-543.
3 Fong Y, Sun RL, Jarnagin W, Blumgart LH: An analysis of 412 cases of hepatocellular carcinoma at a Western center. Ann Surg 1999; 229:790-800.
4 Kiyosawa K, Sodeyama T, Tanaka E, Gibo Y, Yoshizawa K, Nakano Y, Furuta S, Akahane Y, Nishioka K, Purcell RH, Alter HJ: Interrelationship of blood transfusion, non-A, non-B hepatitis and hepatocellular carcinoma: analysis by detection of antibody to hepatitis C virus. Hepatology 1990; 12:671-675.
5 Nishioka K, Watanabe J, Furuta S, Tanaka E, Iino S, Suzuki H, Tsuji T, Yano M, Kuo G, Choo QL, Houghton M, Oda T: A high prevalence of antibody to the hepatitis C virus in patients with hepatocellular carcinoma in Japan. Cancer 1991; 67:429-433.
6 Takenaka K, Yamamoto K, Taketomi A, Itasaka H, Adachi E, Shirabe K, Nishizaki T, Yanaga K, Sugimachi K: A comparison of the surgical results in patients with hepatitis B *versus* hepatitis C-related hepatocellular carcinoma. Hepatology 1995; 22:20-24.
7 Kato Y, Nakata K, Omagari K, Furukawa R, Kusumoto Y, Mori I, Tajima H, Tanioka H, Yano M, Nagataki S: Risk of hepatocellular carcinoma in patients with cirrhosis in Japan. Analysis of infectious hepatitis viruses. Cancer 1994; 74:2234-2238.
8 Koike Y, Shiratori Y, Sato S, Obi S, Teratani T, Imamura M, Hamamura K, Imai Y, Yoshida H, Shiina S, Omata M: Risk factors for recurring hepatocellular carcinoma differ according to infected hepatitis virus-an analysis of 236 consecutive patients with a single lesion. Hepatology 2000; 32:1216-1223.
9 Shim J, Kim BH, Kim NH, Dong SH, Kim HJ, Chang YW, Lee JI, Chang R: Clinical features of HBsAg-negative but anti-HBc-positive hepatocellular carcinoma in a hepatitis B virus endemic area. J Gastroenterol Hepatol 2005; 20:746-751.
10 Uchiyama K, Ueno M, Hama T, Kawai M, Tani M, Terasawa H, Ozawa S, Uemura R, Nakase T, Yamaue H: Recurrence of primary hepatocellular carcinoma after hepatectomy--differences related to underlying hepatitis virus species. Hepatogastroenterology 2005; 52:591-595.
11 Yamanaka N, Tanaka T, Tanaka W, Yamanaka J, Yasui C, Kuroda N, Takada M, Okamoto E: Correlation of hepatitis virus serologic status with clinicopathologic features in patients undergoing hepatectomy for hepatocellular carcinoma. Cancer 1997; 79:1509-1515.
12 Yano Y, Yamashita F, Sumie S, Ando E, Fukumori K, Kiyama M, Oyama T, Kuroki S, Kato O, Yamamoto H, Tanaka M, Sata M: Clinical features of hepatocellular carcinoma seronegative for both HBsAg and anti-HCV antibody but positive for anti-HBc antibody in Japan. Am J Gastroenterol 2002; 97:156-161.
13 Expert Panel on Detection, Evaluation, and Treatment of High Blood Cholesterol in Adults: Executive summary of the third report of the national cholesterol education program (ncep) expert panel on detection, evaluation, and treatment of high blood cholesterol in adults (adult treatment panel iii). Jama 2001; 285:2486-2497.
14 Adami HO, Chow WH, Nyren O, Berne C, Linet MS, Ekbom A, Wolk A, McLaughlin JK, Fraumeni JF Jr: Excess risk of primary liver cancer in patients with diabetes mellitus. J Natl Cancer Inst 1996; 88:1472-1477.
15 Caldwell SH, Crespo DM, Kang HS, Al-Osaimi AM: Obesity and hepatocellular carcinoma. Gastroenterology 2004; 127:S97-103.
16 Davila JA, Morgan RO, Shaib Y, McGlynn KA, El-Serag HB: Diabetes increases the risk of hepatocellular carcinoma in the United States: a population based case control study. Gut 2005; 54:533-539.
17 El-Serag HB, Tran T, Everhart JE: Diabetes increases the risk of chronic liver disease and hepatocellular carcinoma. Gastroenterology 2004; 126:460-468.
18 Powell EE, Jonsson JR, Clouston AD: Steatosis: co-factor in other liver diseases. Hepatology 2005; 42:5-13.
19 Brunt EM: Nonalcoholic steatohepatitis. Semin Liver Dis 2004; 24:3-20.
20 Bugianesi E, Leone N, Vanni E, Marchesini G, Brunello F, Carucci P, Musso A, De Paolis P, Capussotti L, Salizzoni M, Rizzetto M: Expanding the natural history of nonalcoholic steatohepatitis: from cryptogenic cirrhosis to hepatocellular carcinoma. Gastroenterology 2002; 123:134-140.
21 Marrero JA, Fontana RJ, Su GL, Conjeevaram HS, Emick DM, Lok AS: NAFLD may be a common underlying liver disease in patients with hepatocellular carcinoma in the United States. Hepatology 2002; 36:1349-1354.
22 Mori S, Yamasaki T, Sakaida I, Takami T, Sakaguchi E, Kimura T, Kurokawa F, Maeyama S, Okita K: Hepatocellular carcinoma with nonalcoholic steatohepatitis. J Gastroenterol 2004; 39:391-396.
23 Powell EE, Cooksley WG, Hanson R, Searle J, Halliday JW, Powell LW: The natural history of nonalcoholic steatohepatitis: a follow-up study of forty-two patients for up to 21 years. Hepatology 1990; 11:74-80.
24 Shimada M, Hashimoto E, Taniai M, Hasegawa K, Okuda H, Hayashi N, Takasaki K, Ludwig J: Hepatocellular carcinoma in patients with non-alcoholic steatohepatitis. J Hepatol 2002; 37:154-160.
25 Zen Y, Katayanagi K, Tsuneyama K, Harada K, Araki I, Nakanuma Y: Hepatocellular carcinoma arising in non-alcoholic steatohepatitis. Pathol Int 2001; 51:127-131.
26 Liver Cancer Study Group of Japan (Eds.): The General Rules for the Clinical and Pathological Study of Primary Liver Cancer. 4th Edition. Tokyo: Kanehara, 2000.
27 Brunt EM, Janney CG, Di Bisceglie AM, Neuschwander-Tetri BA, Bacon BR: Nonalcoholic steatohepatitis: a proposal for grading and staging the histological lesions. Am J Gastroenterol 1999; 94:2467-2474.
28 Weisell RC: Body mass index as an indicator of obesity. Asia Pac J Clin Nutr 2002; 11:S681-684.
29 Freiberg MS, Cabral HJ, Heeren TC, Vasan RS, Curtis Ellison R: Alcohol consumption and the prevalence of the Metabolic Syndrome in the US: a cross-sectional analysis of data from the Third National Health and Nutrition Examination Survey. Diabetes Care 2004; 27:2954-2959.
30 Djousse L, Arnett DK, Eckfeldt JH, Province MA, Singer MR, Ellison RC: Alcohol consumption and metabolic syndrome: does the type of beverage matter? Obes Res 2004; 12:1375-1385.
31 Sanyal AJ: AGA technical review on nonalcoholic fatty liver disease. Gastroenterology 2002; 123:1705-1725.
32 Angulo P: Nonalcoholic fatty liver disease. N Engl J Med 2002; 346:1221-1231.
33 Lang H, Sotiropoulos GC, Domland M, Fruhauf NR, Paul A, Husing J, Malago M, Broelsch CE: Liver resection for hepatocellular carcinoma in non-cirrhotic liver without underlying viral hepatitis. Br J Surg 2005; 92:198-202.

# Pioglitazone Promotes Survival and Prevents Hepatic Regeneration Failure After Partial Hepatectomy in Obese and Diabetic KK-A$^y$ Mice

Tomonori Aoyama,[1,2] Kenichi Ikejima,[1,2] Kazuyoshi Kon,[1] Kyoko Okumura,[1] Kumiko Arai,[1] and Sumio Watanabe[1,2]

**Pathogenesis of metabolic syndrome–related nonalcoholic steatohepatitis (NASH) involves abnormal tissue-repairing responses in the liver. We investigated the effect of pioglitazone, a thiazolidinedione derivative (TZD), on hepatic regenerative responses in obese, diabetic KK-A$^y$ mice. Male KK-A$^y$ mice 9 weeks after birth underwent two-thirds partial hepatectomy (PH) after repeated intragastric injections of pioglitazone (25 mg/kg) for 5 days. Almost half of the KK-A$^y$ mice died within 48 hours of PH; however, mortality was completely prevented in mice pretreated with pioglitazone. In KK-A$^y$ mice, bromodeoxyuridine (BrdU) incorporation to hepatocyte nuclei 48 hours after PH reached only 1%; however, pioglitazone pretreatment significantly increased BrdU-positive cells to 8%. Cyclin D1 was barely detectable in KK-A$^y$ mice within 48 hours after PH. In contrast, overt expression of cyclin D1 was observed 24 hours after PH in KK-A$^y$ mice pretreated with pioglitazone. Hepatic tumor necrosis factor alpha (TNF-α) messenger RNA (mRNA) was tremendously increased 1 hour after PH in KK-A$^y$ mice, the levels reaching ninefold over C57Bl/6 given PH, whereas pioglitazone blunted this increase by almost three-fourths. Pioglitazone normalized hypoadiponectinemia in KK-A$^y$ mice almost completely. Serum interleukin (IL)-6 and leptin levels were elevated extensively 24 hours after PH in KK-A$^y$ mice, whereas the levels were largely decreased in KK-A$^y$ mice given pioglitazone. Indeed, pioglitazone prevented aberrant increases in signal transducers and activators of transcription (STAT)3 phosphorylation and suppressor of cytokine signaling (SOCS)-3 mRNA in the liver in KK-A$^y$ mice. *Conclusion:* These findings indicated that pioglitazone improved hepatic regeneration failure in KK-A$^y$ mice. The mechanism underlying the effect of pioglitazone on regeneration failure most likely involves normalization of expression pattern of adipokines and subsequent cytokine responses during the early stage of PH.** (HEPATOLOGY 2009; 49:1636-1644.)

See Editorial on Page 1427.

Nonalcoholic fatty liver disease (NAFLD) is one of the important manifestations of metabolic syndrome, a clinical entity comprising obesity, hypertension, glucose intolerance, and hyperlipidemia.[1-3] NAFLD includes a spectrum of liver pathology ranging from simple steatosis to nonalcoholic steatohepatitis (NASH), which demonstrates progressive diseases, including advanced hepatic fibrosis and hepatocellular carcinoma.[1-3] Pathogenesis of metabolic syndrome–related NAFLD/NASH involves a variety of environmental and nutritional factors as well as genetic susceptibilities. Among these, insulin resistance is believed to be the most

*Abbreviations: ANOVA, analysis of variance; BrdU, bromodeoxyuridine; ELISA, enzyme-linked immunosorbent assay; IL, interleukin; JAK, Janus kinase; NASH, nonalcoholic steatohepatitis; mRNA, messenger RNA; NAFLD, nonalcoholic fatty liver disease; ObR, leptin receptor; PCNA, proliferating cell nuclear antigen; PH, partial hepatectomy; PPAR, peroxisome proliferator-activated receptor; RT-PCR, reverse transcription polymerase chain reaction; SEM, standard error of the mean; SOCS, suppressor of cytokine signaling; STAT, signal tranducers and activators of transcription; TNF-α, tumor necrosis factor alpha; TZD, thiazolidinedione derivative.*

*From the [1]Department of Gastroenterology, Juntendo University School of Medicine, and [2]Sportology Center, Juntendo University Graduate School of Medicine, Tokyo, Japan.*

*Received July 26, 2008; accepted December 28, 2008.*

*Supported in part by Grant-in-Aid (No. 19590791 to K.I., No. 18390213 to S.W.) and High Technology Research Center Grant from the Ministry of Education, Culture, Sports, Science and Technology of Japan, and grants from Liver Forum in Kyoto (co-sponsored by Viral Hepatitis Research Foundation in Japan and Dainippon Sumitomo Pharma Co. Ltd., to K.I.) and Research Conference on Alcohol and Health (sponsored by Suntory Co. Ltd.).*

profound metabolic abnormality.[4] It is postulated that adipokines, a group of cytokines produced exclusively from adipose tissue (in other words, leptin, adiponectin, resistin, plasminogen activator inhibitor-1), regulate both metabolic balance and progression of hepatic disorder.[4] The mechanisms underlying the disease progression of NASH involve several key biological responses such as excess oxidative stress, alteration in innate immunity, and abnormal tissue repairing responses. Especially, impairment of hepatic regeneration seems to be critical because regeneration failure often results in progression of hepatic fibrogenesis and subsequent carcinogenesis. Indeed, it has been reported that progression of fibrosis is associated with altered regeneration in NAFLD patients.[5]

It has been well documented that various types of hepatic steatosis and steatohepatitis demonstrate poor hepatic regeneration. For instance, poor hepatic regeneration has been demonstrated in experimental models of hepatic steatosis/steatohepatitis such as ob/ob mice and Zucker rats, which carry genetic defects of leptin and its receptor (ObR), respectively.[6,7] These observations suggest that leptin is an important regulator of liver regeneration; however, the role of adipokines in hepatic regenerative responses without defects in leptin/ObR genes has not been well elucidated. Given the evidence that genetic defects in leptin/ObR genes are seldom found in humans, more clinically relevant animal models are required to investigate the pathophysiology and experimental therapeutics of NAFLD/NASH.

KK-A$^y$ mice are a cross-strain of diabetic KK mice[8] and lethal yellow (A$^y$) mice, which carry mutation of the agouti(a) gene in mouse chromosome 2.[9] KK-A$^y$ mice develop maturity-onset obesity, dyslipidemia, and insulin resistance, in part because of the antagonism of melanocortin receptor-4 by ectopic expression of the agouti protein.[9] Importantly, these mice present hyperleptinemia and leptin resistance without defects in the ObR gene, and the expression of adiponectin is conversely downregulated.[10,11] The phenotype of KK-A$^y$ mice, including altered adipokine expression, quite resembles metabolic syndrome in humans, indicating the potential usefulness of this strain as a model of metabolic syndrome–related NASH. Indeed, we have previously demonstrated that KK-A$^y$ mice are more susceptible to experimental steatohepatitis induced by a methionine-deficient, choline-deficient diet.[11]

The current study aimed to clarify the causal relationship between liver regeneration and metabolic background related to obesity, insulin resistance, and expression of adipokines. Here we investigated the changes in hepatic regenerative response in KK-A$^y$ mice after two-thirds partial hepatectomy (PH). Furthermore, we evaluated the effect of a thiazolidinedione derivative (TZD) pioglitazone, which improves insulin resistance through actions as a peroxisome proliferator–activated receptor (PPAR)γ agonist, on regeneration failure in these animals. Through this study, we tested the hypothesis that pioglitazone improves regenerative responses by modulating inflammation and aberrant adipokine expression in a model of metabolic syndrome–related steatohepatitis.

## Materials and Methods

***Animal Experiments and Operative Procedure.*** Male KK-A$^y$ and C57Bl/6 mice 8 weeks after birth were obtained from CLEA Japan Inc. (Tokyo, Japan). Mice were housed in air-conditioned specific pathogen–free animal quarters with lighting from 8:00 AM to 9:00 PM and given unrestricted access to a standard laboratory chow and water for 1 week before and during experiments. All animals received humane care in compliance with the experimental protocol approved by the Committee of Laboratory Animals according to institutional guidelines. C57Bl/6 mice, which are the grandparental strain of KK-A$^y$ mice, were selected as nonobese and nondiabetic controls. Some KK-A$^y$ mice were treated with 25 mg/kg pioglitazone (a gift from Takeda Pharmaceutical Co., Ltd., Tokyo, Japan) or vehicle by intragastric injection once daily for 5 days before operation. After overnight fasting, 70% PH was performed in the mice according to the Higgins and Anderson method.[12] Mortality was observed up to 48 hours after PH. Mice were sacrificed by exsanguinations from inferior vena cava, and wet weight of the whole remaining liver was measured. Some mice were pulse-labeled with a single intraperitoneal injection of bromodeoxyuridine (BrdU; Sigma Chemical Co., St. Louis, MO; 50 mg/kg in phosphate-buffered saline) 2 hours before sacrifice, and liver specimens were fixed in buffered formalin for immunohistochemistry. Serum and liver samples were kept frozen at −80°C until assayed.

*Address reprint request to: Kenichi Ikejima, M.D., Ph.D., F.A.C.P., Associate Professor, Department of Gastroenterology, Juntendo University School of Medicine, 2-1-1 Hongo, Bunkyo-ku, Tokyo, 113-8421 Japan. E-mail: ikejima@juntendo.ac.jp; fax: (81)-3-3813-8862.*



*Published online in Wiley InterScience (www.interscience.wiley.com).*

*DOI 10.1002/hep.22828*

*Potential conflict of interest: Nothing to report.*

**Table 1. Primer Sets for Real-Time RT-PCR**

| Gene (GeneBank Accession) | Primer Sequences | Product Size |
|---|---|---|
| TNF-α | Forward: 5'-AAGCCTGTAGCCCACGTCGTA-3' | 122 bp |
| (NM_013693) | Reverse: 5'-GGCACCACTAGTTGGTTGTCTTTG-3' | |
| SOCS-3 | Forward: 5'-CAATACCTTTGACAAGCGGACTCTC-3' | 146 bp |
| (NM_007707) | Reverse: 5'-TCAAAGCGCAAACAAGTTCCAG-3' | |
| GAPDH | Forward: 5'-AAATGGTGAAGGTCGGTGTG-3' | 108 bp |
| (NM_001001303) | Reverse: 5'-TGAAGGGGTCGTTGATGG-3' | |

***Immunohistochemistry.*** For immunohistochemistry, formalin-fixed and paraffin-embedded tissue sections were deparaffinized and incubated with 3% $H_2O_2$ for 10 minutes. To examine BrdU incorporation to hepatocyte nuclei, tissue sections were incubated with 2N hydrochloric acid for 30 minutes. After blocking with normal horse serum for 60 minutes, tissue sections were incubated with a mouse monoclonal anti-BrdU antibody (DakoCytomation Norden A/S, Glostrup, Denmark). After rinsing the primary antibody, the sections were incubated with secondary biotinylated anti-mouse immunoglobulin G antibody, and the specific binding was visualized with the avidin–biotin complex solution followed by incubation with a 3,3-diaminobenzidine tetrahydrochloride solution using Vectastain Elite ABC kit (Vector Laboratories, Burlingame, CA). BrdU-positive hepatocytes were counted in five 100× fields on each slide to determine the average number BrdU-labeling index (BrdU-positive hepatocytes/total hepatocytes). Expression of proliferating cell nuclear antigen (PCNA) in hepatocytes was evaluated similarly by immunohistochemistry as previously described elsewhere.[13] Specimens were observed and photographed using a microscope (BH-2, Olympus Corp., Tokyo, Japan) equipped with a digital imaging system (VB-6010, Keyence Corp., Osaka, Japan).

***Western Blot Analysis.*** Whole-liver protein extracts were prepared by homogenizing frozen tissue in a buffer containing 50 mM Tris-hydrochloric acid (pH 8.0), 150 mM sodium chloride, 1 mM ethylenediaminetetraacetic acid, 1% Triton X-100, protease inhibitors (Complete Mini, Roche Diagnostics Co., Mannheim, Germany), and a phosphatase inhibitor $Na_3VO_4$ (50 μM, Sigma Chemical Co.), followed by a centrifugation at 10,400 g for 10 minutes. Protein concentration was determined by Bradford assay using Bio-Rad protein assay kit (Bio-Rad Laboratories, Hercules, CA). Fifty micrograms protein was separated in 10% to 15% sodium dodecyl sulfate polyacrylamide gel electrophoresis and electrophoretically transferred onto polyvinylamide fluoride membranes. After blocking with 5% nonfat dry milk in Tris-buffered saline, membranes were incubated overnight at 4°C with rabbit polyclonal anti-cyclin D1, anti-phospho-signal tranducers and activators of transcription 3 (STAT3) (Tyr705) or anti-STAT3 (Cell Signaling Technology Inc., Beverly, MA), followed by a secondary horseradish peroxidase–conjugated anti-rabbit immunoglobulin G antibody (DakoCytomation Norden A/S). Subsequently, specific bands were visualized using the enhanced chemiluminescence detection kit (Amersham Pharmacia Biotech, Piscataway, NJ).

***Measurement of Blood Glucose and Enzyme-Linked Immunosorbent Assay.*** Blood glucose levels were measured enzymatically using standard glucose test strips and a glucometer (Glutest Sensor and Glutest Ace; Sanwa Kagaku Kenkyusho Co. Ltd., Nagoya, Japan). Serum insulin, adiponectin, interleukin (IL)-6, and leptin were determined using enzyme-linked immunosorbent assay (ELISA) kits (insulin and leptin: Seikagaku Corp., Tokyo, Japan; adiponectin: Otsuka Pharmaceutical Co.Ltd., Tokyo, Japan; IL-6: eBiocience, San Diego, CA) according to the manufacturer's instruction.

***RNA Preparation and Real-Time Reverse Transcription Polymerase Chain Reaction.*** Total liver RNA was prepared from frozen tissue samples by guanidium/cesium trifluoroacetete extraction method using Quick Prep total RNA extraction kit (Amersham Pharmacia Biotech). The concentration and purity of isolated RNA were determined by measuring optical density at 260 and 280 nm. Furthermore, the integrity of RNA was verified by electrophoresis on formaldehyde denaturing agarose gels.

For real-time reverse transcription polymerase chain reaction (RT-PCR), total RNA (1 μg) was reverse-transcribed using Moloney murine leukemia virus transcriptase (Super-Script II, Invitrogen Corp., Carlsbad, CA) and a deoxythymidine oligonucleotides [oligo(dT)12-18] primer (Invitrogen Corp.) at 42°C for 1 hour. Obtained complementary DNA (1 μg) was amplified using SYBR Premix Ex TaqTM (Takara Bio, Tokyo, Japan) and specific primers as appropriate. Primer sets for tumor necrosis factor alpha (TNF-α), suppressor of cytokine signaling 3 (SOCS3), and glyceraldehyde-3-phosphate dehydrogenase are shown in Table 1. After a 10-second activation period at 95°C, 40 cycles of 95°C for 5 seconds, and 60°C

for 31 seconds, followed by the final cycle of 95°C for 15 seconds, 60°C for 1 minute, and 95°C for 15 seconds, were performed using ABI Prism 7700 Sequence Detection System (PE Applied Biosystems, Foster City, CA), and the threshold cycle ($C_T$) values were obtained.

***Image and Statistical Analysis.*** Densitometrical analysis was performed using Scion Image (version Beta 4.0.2, Scion Corp., Frederick, MD). Data were expressed as means ± standard error of the mean (SEM). Statistical differences between means were determined using Mann-Whitney rank sum test or analysis of variance (ANOVA) on ranks followed by a post hoc test (Student-Newman-Keuls all pairwise comparison procedures) as appropriate. Statistical significance for percent survival was determined by log-rank test. A value of $P < 0.05$ was selected before the study to reflect significance.

## Results

***Liver Regeneration After PH Is Impaired in KK-A$^y$ Mice.*** In this study, we first investigated the strain differences in liver regeneration after 70% PH between KK-A$^y$ mice and C57Bl/6 mice as controls. Because impaired liver regeneration often results in death, we observed the mortality after PH in both strains of mice (Fig. 1A). All of the C57Bl/6 mice were alive after PH as expected; however, 50% of KK-A$^y$ mice died within 48 hours after PH. In C57Bl/6 mice, the wet weight of the remnant liver was increased 2.1-fold within 48 hours; in contrast, the values were only 1.4-fold in KK-A$^y$ mice (Fig. 1B). To evaluate DNA synthesis during liver regeneration, we next examined BrdU uptake into hepatocyte nuclei by immunohistochemistry (Fig. 1C-E). BrdU incorporation was observed in 22% of hepatocytes 48 hours after PH in C57Bl/6 mice; however, the levels only reached 1% in KK-A$^y$ mice given the same procedure. To further confirm the impaired regeneration in KK-A$^y$ mice, hepatic expression of cyclin D1 was detected by western blotting (Fig. 2). In C57Bl/6 mice, cyclin D1 expression was increased almost ninefold over basal levels 48 hours after PH; however, KK-A$^y$ mice almost completely lacked increases in cyclin D1 after PH. Taken together, these findings clearly indicated that KK-A$^y$ mice demonstrate extremely poor regenerating response in the liver after PH.

***Effect of Pioglitazone on Liver Regeneration After PH in KK-A$^y$ Mice.*** We next investigated the effect of pioglitazone on regeneration failure and mortality after PH in KK-A$^y$ mice. Interestingly, the mortality after PH was completely prevented in KK-A$^y$ mice given pioglitazone for 5 consecutive days before operation (Fig. 3A). Pioglitazone pretreatment significantly increased BrdU-positive hepatocytes in KK-A$^y$ mice 48 hours after PH to 7.2% (Fig. 3B, C, F). Similarly, pioglitazone increased the

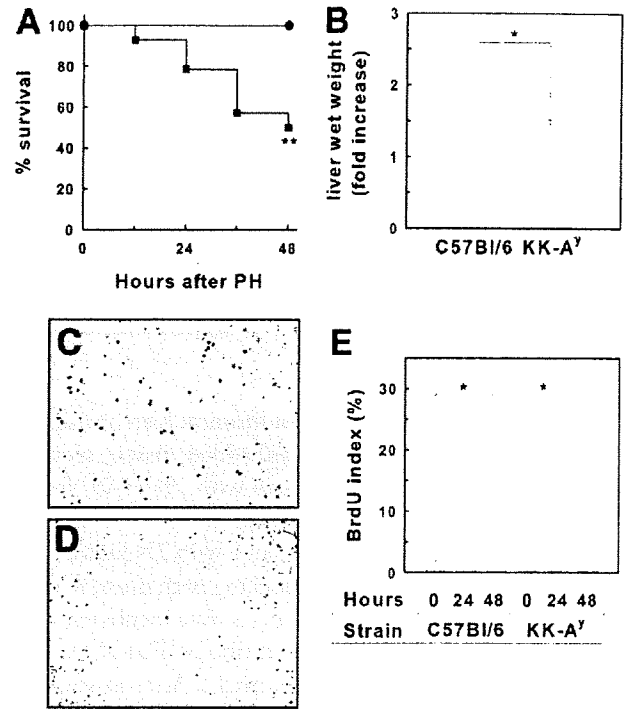


Fig. 1. Impaired liver regeneration after PH in KK-A$^y$ mice. Both C57Bl/6 and KK-A$^y$ mice underwent 70% partial hepatectomy (PH). Percentages of survival in C57Bl/6 controls (closed circle) and KK-Ay mice (closed square) up to 48 hours after PH are plotted (A; n = 14; $*P < 0.05$ versus C57Bl/6 by log-rank test). Wet weight of the liver was measured before and 48 hours after PH (B; n = 5; $*P < 0.05$, by Mann-Whitney rank-sum test). Representative photomicrographs of BrdU staining 48 hours after PH from C57Bl/6 (C) and KK-A$^y$ mice (D) are shown (original magnification 100×). Mean BrdU indices are plotted (E; n = 5; mean ± SEM, $*P < 0.05$, by ANOVA on ranks and Student-Newman-Keuls post-hoc test).

percentages of PCNA-positive hepatocytes almost 10-fold in KK-A$^y$ mice 48 hours after PH (Fig. 3D-E, G). Furthermore, overt expression of cyclin D1 was observed 24 hours after PH in KK-A$^y$ mice when they were pretreated with pioglitazone (Fig. 4A, B), confirming that pioglitazone improves liver regeneration failure after PH in these mice.

***Effect of Pioglitazone on Blood Glucose/Insulin Regulation After PH in KK-A$^y$ Mice.*** Because one of the characteristic phenotypes of KK-Ay mice is glucose intolerance, we monitored blood glucose levels during the time course of PH (Fig. 5A). Fasting blood glucose levels in KK-A$^y$ mice are significantly higher than those in C57Bl/6 mice as expected, the values being 177.8 ± 3.9 and 80.8 ± 6.2 mg/dL, respectively. Pretreatment with pioglitazone decreased fasting blood glucose levels in KK-A$^y$ mice to values reaching 122.2 ± 11.4 mg/dL. Blood glucose levels in C57Bl/6 mice were slightly increased after PH and maintained the levels around

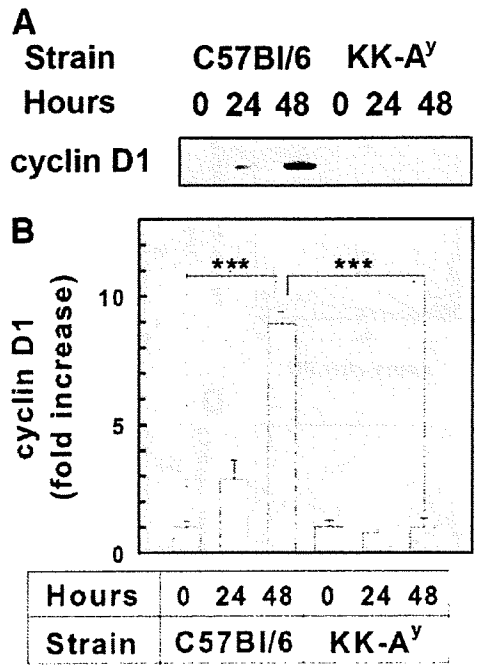


Fig. 2. Hepatic cyclin D1 expression after PH. Experimental designs as in Fig. 1. Expression of cyclin D1 in the liver was detected by western blotting. Representative photographs of specific bands from five individual experiments are shown (A). The densitometrical results for cyclin D1 (expressed as fold over C57Bl/6 controls) are plotted (B; n = 5; mean ± SEM, ***$P < 0.001$, by one-way ANOVA and Student-Newman-Keuls post-hoc test).

118.8 ± 8.9 mg/dL up to 48 hours after PH. In sharp contrast, blood glucose levels in KK-A$^y$ mice were drastically degreased after PH, the values being as low as 58.8 ± 8.1mg/dL at 48 hours. Interestingly, pioglitazone pretreatment paradoxically prevented this hypoglycemia with values of 113.6 ± 2.0 mg/dL at 48 hours after PH.

Next, we measured serum insulin levels in these animals (Fig. 5B). Fasting serum insulin levels in KK-A$^y$ mice were significantly higher than those in C57Bl/6 mice, the levels being 1.64 ± 0.25 and 0.13 ± 0.03 ng/mL, respectively (Fig. 5B). Pioglitazone pretreatment decreased fasting serum insulin levels in KK-A$^y$ mice to the values of 0.43 ± 0.06 ng/mL. After PH, serum insulin levels in C57Bl/6 mice were slightly elevated in 3 hours to the values of 0.7 ± 0.05 ng/mL, and kept constant levels thereafter. In sharp contrast, serum insulin levels in KK-A$^y$ mice were tremendously increased after PH, with maximum values of 16.6 ± 6.1 ng/mL 12 hours after PH. In KK-A$^y$ mice pretreated with pioglitazone, increases in serum insulin levels after PH were significantly blunted as compared with those in mice without pioglitazone, with the peak values reaching only 4.13 ± 1.29 ng/mL at 24 hours.

***Effects of Pioglitazone on Hepatic TNF-α Messenger RNA and Serum Adiponectin, IL-6, and Leptin Levels After PH in KK-A$^y$ Mice.*** Because TNF-α is believed to promote liver regeneration in the early phase,[14,15] hepatic TNF-α messenger RNA (mRNA) were measured by real-time RT-PCR (Fig. 6A). TNF-α mRNA levels in the liver before PH were quite low, and no difference was observed between two strains. After PH, hepatic TNF-α mRNA was swiftly increased with a single, small peak within 1 hour in C57Bl/6 mice as expected. In contrast, increases in TNF-α mRNA 1 hour after PH were greatly enhanced, with the maximal levels reaching almost ninefold over C57Bl/6 peaks, followed by the second peak 24 hours later. Pretreatment with

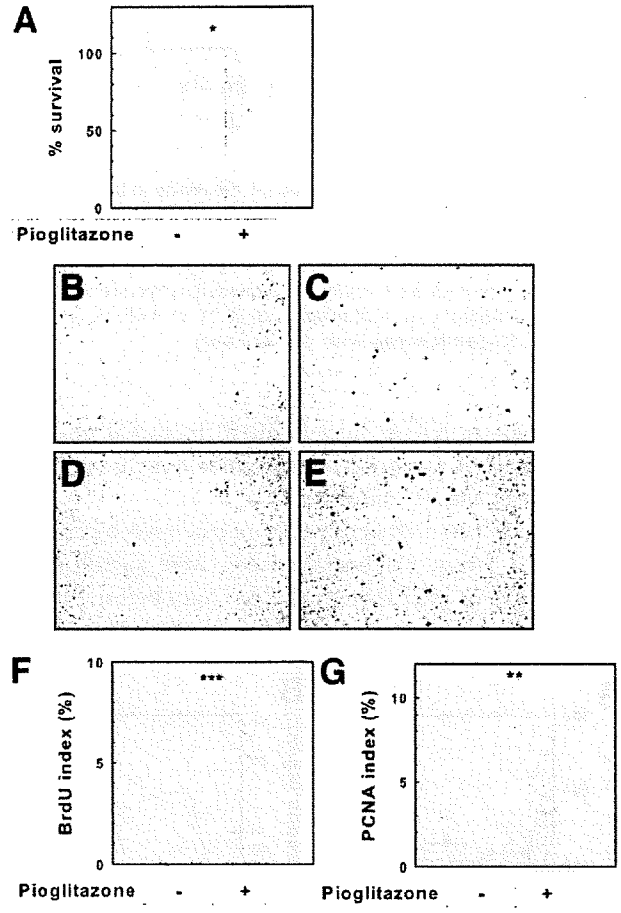


Fig. 3. Effect of pioglitazone on liver regeneration after PH in KK-A$^y$ mice. KK-A$^y$ mice pretreated with pioglitazone or vehicle alone underwent 70% PH, and mortality was observed up to 48 hours later. Percentages of survival are plotted (A; n = 10; *$P < 0.05$ by log-rank test). Representative photomicrographs of BrdU (B, C) and PCNA (D, E) staining 48 hours after PH from KK-A$^y$ mice pretreated with vehicle alone (left panels; B, D) and pioglitazone (right panels; C, E) are shown (original magnification 100×). Mean indices of BrdU (F) and PCNA (G) in each group are plotted (n = 5; mean ± SEM, ***$P < 0.001$, by Mann-Whitney rank-sum test).

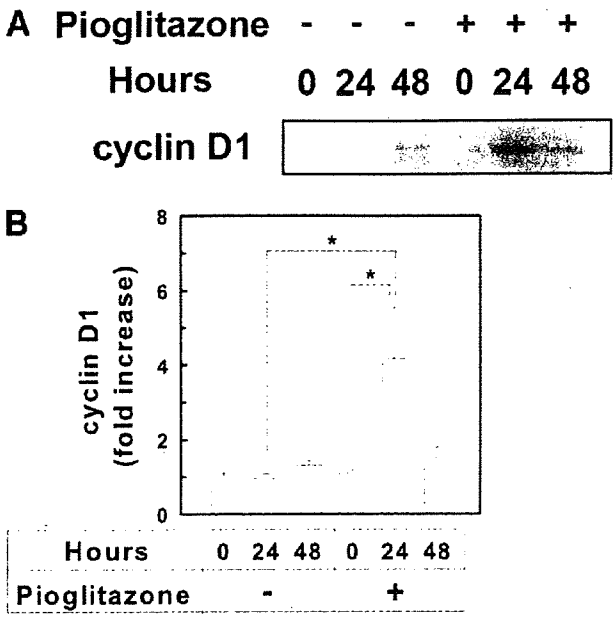


Fig. 4. Effect of pioglitazone on cyclin D1 expression in the liver after PH in KK-A$^y$ mice. Experimental designs as in Fig. 3. Expression of cyclin D1 in the liver was detected by western blotting. Representative photographs of specific bands from five individual experiments are shown (A). The densitometrical results for cyclin D1 (expressed as fold over C57Bl/6 controls) are plotted (B; n = 5; mean ± SEM, *$P < 0.05$, by one-way ANOVA and Student-Newman-Keuls post-hoc test).

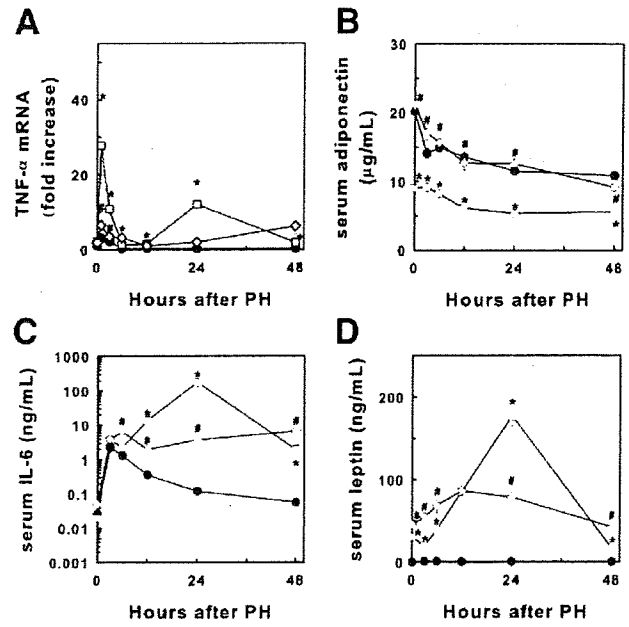


Fig. 6. Effects of pioglitazone on hepatic TNF-α mRNA and serum adiponectin, IL-6, and leptin levels after PH in KK-A$^y$ mice. The levels of TNF-α mRNA in the liver (A) were determined by real-time RT-PCR, and serum adiponectin (B), IL-6 (C), and leptin (D) levels were measured by ELISA. These parameters in C57Bl/6 mice (closed circle), KK-A$^y$ mice (open square), and KK-A$^y$ mice pretreated with pioglitazone (gray diamond) are plotted (n = 5; mean ± SEM, *$P < 0.05$ versus C57Bl/6 mice, #$P < 0.05$ versus KK-A$^y$ mice in each time point by ANOVA on ranks and Student-Newman-Keuls post-hoc test).

pioglitazone to KK-A$^y$ mice blunted the initial peak of TNF-α mRNA by approximately three fourths, and the second peak almost completely.

Next, we measured serum adiponectin levels by ELISA (Fig. 6B). Serum adiponectin levels were significantly lower in KK-A$^y$ mice than in C57Bl6 mice before PH, as expected. In both strains of mice, serum adiponectin levels tended to decrease gradually after PH; however, the levels in KK-A$^y$ mice were lower than those in C57Bl/6 mice throughout the time course after PH. Interestingly, hypoadiponectinemia observed in KK-A$^y$ mice was reversed by pioglitazone pretreatment almost completely. Serum adiponectin levels in KK-A$^y$ mice pretreated with pioglitazone were almost similar to C57Bl/6 controls in all times after PH.

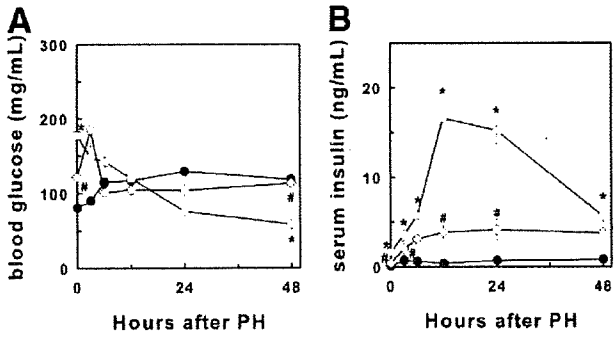


Fig. 5. Effect of pioglitazone on blood glucose and serum insulin levels after PH in KK-A$^y$ mice. Blood glucose levels were detected enzymatically, and serum insulin levels were measured by ELISA. Mean blood glucose levels (A) and serum insulin levels (B) in C57Bl/6 mice (closed circle), KK-A$^y$ mice (open square), and KK-A$^y$ mice pretreated with pioglitazone (gray diamond) are plotted (n = 5; mean ± SEM, *$P < 0.05$ versus C57Bl/6 mice, #$P < 0.05$ versus KK-A$^y$ mice in each time point by ANOVA on ranks and Student-Newman-Keuls post-hoc test).

IL-6 and the Janus kinase (JAK)-STAT pathway also play a pivotal role in liver regeneration[16,17]; therefore, we measured serum IL-6 levels after PH by ELISA (Fig. 6 C). In C57Bl/6 mice, serum IL-6 levels peaked at 3 hours after PH with values reaching 2.3 ± 0.7 ng/mL, and then decreased thereafter. In KK-A$^y$ mice, serum IL-6 levels were drastically elevated, with maximal values of 178.3 ± 38.9 ng/mL at 24 hours after PH. In contrast, pioglitazone pretreatment significantly blunted this increase in serum IL-6 after PH in KK-A$^y$ mice almost completely.

Because leptin shares the same JAK-STAT pathway through Ob-Rb, which is predominantly expressed in sinusoidal cells in the liver,[18] we also measured serum leptin levels after PH in KK-A$^y$ mice (Fig. 6D). Serum leptin levels in untreated KK-A$^y$ mice were remarkably high

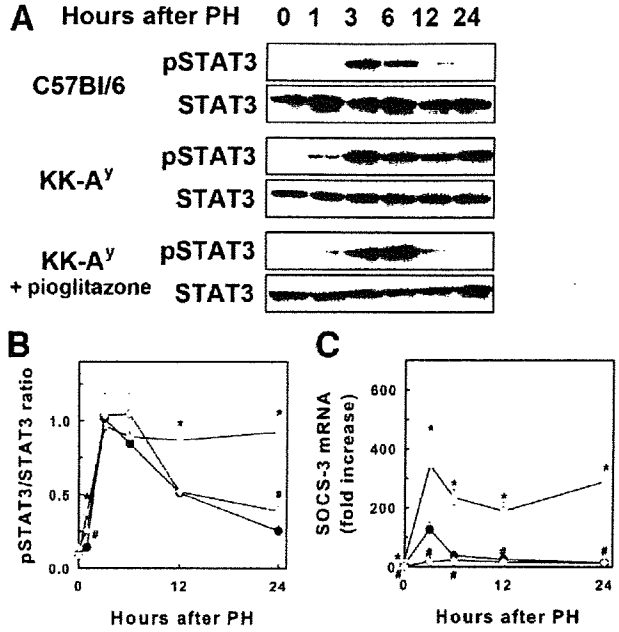


Fig. 7. Effects of pioglitazone on phosphorylation of STAT3 and SOCS-3 mRNA in the liver after PH in KK-A$^y$ mice. Phosphorylation of STAT3 and SOCS-3 mRNA in the liver were detected by western blotting and real-time RT-PCR, respectively. Representative photographs of specific bands for phospho (p)-STAT3, and total STAT3 from five individual experiments are shown (A). The densitometrical results for pSTAT3/STAT3 ratio (B) and hepatic SOCS-3 mRNA levels (C) in C57Bl/6 mice (closed circle), KK-A$^y$ mice (open square), and KK-A$^y$ mice pretreated with pioglitazone (gray diamond) are plotted (n = 5; mean ± SEM, $*P <$ 0.05 versus C57Bl/6 mice, $\#P < 0.05$ versus KK-A$^y$ mice in each time point by ANOVA on ranks and Student-Newman-Keuls post-hoc test).

compared with the levels in C57Bl/6 controls, as expected. In KK-A$^y$ mice pretreated with pioglitazone, serum leptin levels before PH were further increased to 45.4 ± 3.1 ng/mL. In C57Bl/6 mice, serum leptin levels were slightly elevated 3 hours after PH to values of 1.0 ± 0.2 ng/mL, and sustained until 48 hours. In sharp contrast, serum leptin levels were tremendously increased in KK-A$^y$ mice, with maximal values of 176.9 ± 13.7 ng/mL 24 hours after PH. Pioglitazone pretreatment blunted the peak serum leptin levels in hepatectomized KK-A$^y$ mice by almost half, with a shifted peak time to 12 hours after PH.

***Effects of Pioglitazone on Phosphorylation of STAT3 and SOCS-3 mRNA in the Liver After PH in KK-A$^y$ Mice.*** Because remarkable differences were observed in serum IL-6 and leptin levels after PH, we further investigated the activation of the downstream JAK-STAT pathway by detecting phosphorylation of STAT3 (Tyr705) in the liver, using western blot analysis (Fig. 7A, B). In C57Bl/6 mice, the levels of STAT3 phosphorylation in the liver were increased 3 hours after PH, followed by a gradual decrease to near basal levels within 24 hours. Hepatic phospho-STAT3 levels in KK-A$^y$ mice were also elevated 3 hours after PH but sustained persistently until 24 hours later. Pioglitazone pretreatment, however, inhibited this sustained increase in phospho-STAT3 in KK-A$^y$ mice almost completely.

Finally, we evaluated mRNA levels of SOCS-3, a negative regulator of the JAK-STAT pathway, in the liver by real-time RT-PCR (Fig. 7C). In C57Bl/6 mice, hepatic SOCS-3 mRNA levels were increased 3 hours after PH, followed by gradual decrease to near basal levels at 24 hours. In KK-A$^y$ mice that received PH, the peak levels at 3 hours were almost 2.8-fold higher than those in C57Bl/6 mice, and the higher levels of SOCS-3 mRNA were thereafter sustained until 24 hours after PH. Pioglitazone pretreatment, however, prevented increases in hepatic SOCS-3 mRNA in KK-A$^y$ mice almost completely throughout the time course after PH. Taken together, these findings indicated that pretreatment with pioglitazone normalizes the pattern of the JAK-STAT signal activation in KK-A$^y$ mice after PH.

## Discussion

Hepatic regeneration is one of the most typical and well-characterized tissue-repairing responses in the mammalian body.[16,17] Under normal conditions, two-thirds PH in rodents is not lethal, and the remnant liver spontaneously regenerates to regain the original organ size with proper functions within several days. However, hepatic regeneration is impaired in the fatty liver in various genetically obese animals such as ob/ob mice and Zucker (fa/fa) rats.[6,7] In the current study, we demonstrated that KK-A$^y$ mice, which present obese and diabetic phenotypes, also lack normal hepatic regenerative response, with increased mortality after two-thirds PH (Figs. 1, 2). It is striking that pioglitazone, a TZD, not only prevented hepatic regeneration failure but also promoted survival after PH in KK-A$^y$ mice almost completely (Figs. 3, 4).

Regarding the mechanisms of regeneration failure, KK-A$^y$ mice demonstrated some outstanding abnormal responses after PH. First, KK-A$^y$ mice showed excessive induction of TNF-$\alpha$ mRNA in the liver (Fig. 6A). Although TNF-$\alpha$ produced by Kupffer cells plays an important role in the initiation of normal hepatic regeneration,[14,19] excess induction of TNF-$\alpha$ in Kupffer cells might interfere with the regenerative responses. Indeed, we confirmed that BrdU incorporation in the liver 48 hours after PH in C57Bl/6 mice was blunted significantly by simultaneous treatment with recombinant TNF-$\alpha$ (data not shown). In KK-A$^y$ mice, augmented TNF-$\alpha$ production seems to inhibit regeneration without inducing apparent hepatocellular injury, because no obvious increases in apoptotic hepatocytes were detected after PH by using M30 CytoDEATH immunohisto-

chemistry (Roche Diagnostics Co.), which visualizes caspase cleavage product of cytokeratin 18 (data not shown). Conversely, adiponectin has been shown to inhibit lipopolysaccharide induction of macrophage activation both in vitro and *in vivo*.[10,20] Because KK-A$^y$ mice present significant hypoadiponectinemia (Fig. 6B), it is reasonable that Kupffer cells in these animals are more susceptible to certain stimuli such as gut-derived endotoxin (lipopolysaccharide). In contrast, mice pretreated with pioglitazone showed nearly normal serum adiponectin levels (Fig. 6B), which most likely prevented excess production of TNF-$\alpha$ from Kupffer cells during regeneration in KK-A$^y$ mice. It is also possible that pioglitazone inhibits activation of Kupffer cells independent of adiponectin, because it has also been reported that TZDs inhibit activation of Kupffer cells in a direct manner.[21,22] Taken together, these findings support the hypothesis that the abnormal innate immune responses are critical for the regeneration failure in KK-A$^y$ mice.

Second, KK-A$^y$ mice showed remarkable increases in serum IL-6 and leptin levels after PH (Fig. 6C, D), which share the same intracellular signaling pathway involving JAK-STAT3. Given the evidence that IL-6, leptin, and the JAK-STAT signals play a pivotal role in liver regeneration,[23-26] it is conceivable that dysregulation in JAK-STAT signaling is profoundly involved in regeneration failure observed in KK-A$^y$ mice. The role of IL-6 and the JAK-STAT pathway in hepatic regeneration, however, appears to be complex. Knockout mice deficient in IL-6 have been shown to lack hepatocyte proliferation after PH,[23] whereas mice lacking its receptor glycoprotein (gp)130 demonstrate only minor changes in cell cycle and DNA synthesis in hepatocytes after PH.[27] In this study, we demonstrated that increases in phospho-STAT3, as well as the induction of SOCS-3 mRNA, in the hepatectomized liver were sustained in KK-A$^y$ mice (Fig. 7). Furthermore, pretreatment with pioglitazone normalized phosphorylation of STAT3 (Fig. 7A, B) and increased cyclin D1 expression after PH in KK-A$^y$ mice. Because the JAK-STAT pathway is involved in tissue protection in various kinds of hepatic injuries,[28,29] up-regulation of the JAK-STAT signaling in KK-A$^y$ mice is considered as a stress-related protective response in the liver. Importantly, it has been reported that excess phosphorylation of STAT3 results in poor hepatic regeneration because of direct down-regulation of cyclin D1 expression[26,30,31] and that higher SOCS-3 expression in hepatocytes lacking gp130-dependent Ras correlates with delayed hepatocyte proliferation.[32] Collectively, these findings are consistent with the hypothesis that sustained activation of the JAK-STAT pathway leads to inhibition of cyclin D1, thereby causing regeneration failure in KK-A$^y$ mice.

It is not clear whether the increase in mortality in KK-A$^y$ mice is caused by hepatic failure after PH; however, it is obvious that KK-A$^y$ mice developed progressive hypoglycemia after PH, even though they showed significant hyperglycemia before operation (Fig. 5A). In fact, KK-A$^y$ mice showed extremely high serum insulin levels after PH (Fig. 5B), and it is considerable that the liver in KK-A$^y$ mice failed to provide adequate amount of glucose by inhibiting glycogenesis and facilitating gluconeogenesis. In this aspect, the mortality after PH in KK-A$^y$ mice, especially in the late phase, might be attributable to impaired glucose metabolism. Interestingly, pretreatment with pioglitazone, an insulin sensitizer, paradoxically prevents hypoglycemia after PH in KK-A$^y$ mice (Fig. 5A). This is also consistent with the fact that pioglitazone blunted increases in serum insulin levels after PH (Fig. 5B). It is postulated that pioglitazone normalizes serum adiponectin levels, thereby avoiding irregular increases in serum insulin levels and subsequent hypoglycemia, thus in part promoting survival, after PH in KK-A$^y$ mice.

PPAR-$\gamma$ is a key nuclear receptor/transcription factor for transcriptional regulation of various genes related to glucose/lipid metabolism, immune responses, and tissue repair.[33] Because TZDs, synthetic PPAR-$\gamma$ ligands, not only improve insulin resistance but also inhibit activation of Kupffer cells[21,22] and transactivation of hepatic stellate cells,[34-36] these chemicals are believed to be suitable for prevention/treatment of hepatic inflammation and fibrogenesis in NASH. Indeed, a placebo-controlled randomized study has demonstrated the therapeutic efficacy of pioglitazone on NASH in terms of both metabolic and histological improvement.[37] It has been reported that TZDs rather inhibit liver regeneration after PH in normal rodents.[38,39] It is important to note, however, that TZDs are regularly applied for pathophysiological conditions involving insulin resistance. Our data added new experimental evidence that pioglitazone prevents hepatic regeneration failure in steatohepatitis. In metabolic syndrome–related steatohepatitis, such as in KK-A$^y$ mice, pioglitazone most likely exerts beneficial effects, rather than inhibitory actions, on hepatic regeneration failure. It is postulated that therapeutic effects of pioglitazone on NASH in part involve normalization of tissue repairing responses in the liver.

In conclusion, KK-A$^y$ mice, which present phenotypes resembling metabolic syndrome in humans, demonstrated severe hepatic regeneration failure with high mortality after PH. This regeneration failure was prevented partially, and the mortality was completely prevented by pretreatment with pioglitazone. The mechanisms underlying the regeneration failure in KK-A$^y$ mice most likely involve alteration in innate immune responses and abnormal JAK-STAT signaling based on imbalance of adipo-

kine expression. Pioglitazone improves the expression pattern of adipokines and normalizes innate immune responses and the aberrant JAK-STAT signaling, thereby facilitating regenerative responses in KK-A$^y$ mice. These findings add a new aspect of therapeutic advantages of pioglitazone for treatment of NASH.

## References


1. Angulo P. Nonalcoholic fatty liver disease. N Engl J Med 2002;346:1221-1231.
2. Clark JM, Brancati FL, Diehl AM. Nonalcoholic fatty liver disease. Gastroenterology 2002;122:1649-1657.
3. Watanabe S, Yaginuma R, Ikejima K, Miyazaki A. Liver diseases and metabolic syndrome. J Gastroenterol 2008;43:509-518.
4. Tilg H, Hotamisligil GS. Nonalcoholic fatty liver disease: cytokine-adipokine interplay and regulation of insulin resistance. Gastroenterology 2006; 131:934-945.
5. Richardson MM, Jonsson JR, Powell EE, Brunt EM, Neuschwander-Tetri BA, Bhathal PS, et al. Progressive fibrosis in nonalcoholic steatohepatitis: association with altered regeneration and a ductular reaction. Gastroenterology 2007;133:80-90.
6. Yang SQ, Lin HZ, Mandal AK, Huang J, Diehl AM. Disrupted signaling and inhibited regeneration in obese mice with fatty livers: implications for nonalcoholic fatty liver disease pathophysiology. HEPATOLOGY 2001;34: 694-706.
7. Picard C, Lambotte L, Starkel P, Sempoux C, Saliez A, Van den Berge V. Steatosis is not sufficient to cause an impaired regenerative response after partial hepatectomy in rats. J Hepatol 2002;36:645-652.
8. Iwatsuka H, Shino A, Suzuoki Z. General survey of diabetic features of yellow KK mice. Endocrinol Jpn 1970;17:23-35.
9. Miller MW, Duhl DM, Vrieling H, Cordes SP, Ollmann MM, Winkes BM, et al. Cloning of the mouse agouti gene predicts a secreted protein ubiquitously expressed in mice carrying the lethal yellow mutation. Genes Dev 1993;7:454-467.
10. Masaki T, Chiba S, Tatsukawa H, Yasuda T, Noguchi H, Seike M, et al. Adiponectin protects LPS-induced liver injury through modulation of TNF-alpha in KK-Ay obese mice. HEPATOLOGY 2004;40:177-184.
11. Okumura K, Ikejima K, Kon K, Abe W, Yamashina S, Enomoto N, et al. Exacerbation of dietary steatohepatitis and fibrosis in obese, diabetic KK-A(y) mice. Hepatol Res 2006;36:217-228.
12. Higgins GM, Anderson RM. Experimental pathology of the liver. Arch Pathol 1931;12:186-202.
13. Abe W, Ikejima K, Lang T, Okumura K, Enomoto N, Kitamura T, et al. Low molecular weight heparin prevents hepatic fibrogenesis caused by carbon tetrachloride in the rat. J Hepatol 2007;46:286-294.
14. Akerman P, Cote P, Yang SQ, McClain C, Nelson S, Bagby GJ, et al. Antibodies to tumor necrosis factor-alpha inhibit liver regeneration after partial hepatectomy. Am J Physiol 1992;263:G579-G585.
15. Yamada Y, Webber EM, Kirillova I, Peschon JJ, Fausto N. Analysis of liver regeneration in mice lacking type 1 or type 2 tumor necrosis factor receptor: requirement for type 1 but not type 2 receptor. HEPATOLOGY 1998: 28:959-970.
16. Taub R. Liver regeneration: from myth to mechanism. Nat Rev Mol Cell Biol 2004;5:836-847.
17. Fausto N, Campbell JS, Riehle KJ. Liver regeneration. HEPATOLOGY 2006: 43(Suppl 1):S45-S53.
18. Ikejima K, Takei Y, Honda H, Hirose M, Yoshikawa M, Zhang YJ, Lang T, et al. Leptin receptor-mediated signaling regulates hepatic fibrogenesis and remodeling of extracellular matrix in the rat. Gastroenterology 2002; 122:1399-1410.
19. Diehl AM, Yang SQ, Yin M, Lin HZ, Nelson S, Bagby G. Tumor necrosis factor-alpha modulates CCAAT/enhancer binding proteins-DNA binding activities and promotes hepatocyte-specific gene expression during liver regeneration. HEPATOLOGY 1995;22:252-261.
20. Matsumoto H, Tamura S, Kamada Y, Kiso S, Fukushima J, Wada A, et al. Adiponectin deficiency exacerbates lipopolysaccharide/D-galactosamine-induced liver injury in mice. World J Gastroenterol 2006;12:3352-3358.
21. Uchimura K, Nakamuta M, Enjoji M, Irie T, Sugimoto R, Muta T, et al. Activation of retinoic X receptor and peroxisome proliferator-activated receptor-gamma inhibits nitric oxide and tumor necrosis factor-alpha production in rat Kupffer cells. HEPATOLOGY 2001;33:91-99.
22. Enomoto N, Takei Y, Hirose M, Konno A, Shibuya T, Matsuyama S, et al. Prevention of ethanol-induced liver injury in rats by an agonist of peroxisome proliferator-activated receptor-gamma, pioglitazone. J Pharmacol Exp Ther 2003;306:846-854.
23. Cressman DE, Greenbaum LE, DeAngelis RA, Ciliberto G, Furth EE, Poli V, et al. Liver failure and defective hepatocyte regeneration in interleukin-6-deficient mice. Science 1996;274:1379-1383.
24. Streetz KL, Luedde T, Manns MP, Trautwein C. Interleukin 6 and liver regeneration. Gut 2000;47:309-312.
25. Wustefeld T, Rakemann T, Kubicka S, Manns MP, Trautwein C. Hyperstimulation with interleukin 6 inhibits cell cycle progression after hepatectomy in mice. HEPATOLOGY 2000;32:514-522.
26. Leclercq IA, Field J, Farrell GC. Leptin-specific mechanisms for impaired liver regeneration in ob/ob mice after toxic injury. Gastroenterology 2003; 124:1451-1464.
27. Wuestefeld T, Klein C, Streetz KL, Betz U, Lauber J, Buer J, et al. Interleukin-6/glycoprotein 130-dependent pathways are protective during liver regeneration. J Biol Chem 2003;278:11281-11288.
28. Streetz KL, Tacke F, Leifeld L, Wustefeld T, Graw A, Klein C, et al. Interleukin 6/gp130-dependent pathways are protective during chronic liver diseases. HEPATOLOGY 2003;38:218-229.
29. Klein C, Wustefeld T, Assmus U, Roskams T, Rose-John S, Muller M, et al. The IL-6-gp130-STAT3 pathway in hepatocytes triggers liver protection in T cell-mediated liver injury. J Clin Invest 2005;115:860-869.
30. Torbenson M, Yang SQ, Liu HZ, Huang J, Gage W, Diehl AM. STAT-3 overexpression and p21 up-regulation accompany impaired regeneration of fatty livers. Am J Pathol 2002;161:155-161.
31. Matsui T, Kinoshita T, Hirano T, Yokota T, Miyajima A. STAT3 down-regulates the expression of cyclin D during liver development. J Biol Chem 2002;277:36167-36173.
32. Dierssen U, Beraza N, Lutz HH, Liedtke C, Ernst M, Wasmuth HE, et al. Molecular dissection of gp130-dependent pathways in hepatocytes during liver regeneration. J Biol Chem 2008;283:9886-9895.
33. Michalik L, Wahli W. Involvement of PPAR nuclear receptors in tissue injury and wound repair. J Clin Invest 2006;116:598-606.
34. Miyahara T, Schrum L, Rippe R, Xiong S, Yee HF Jr, Motomura K, et al. Peroxisome proliferator-activated receptors and hepatic stellate cell activation. J Biol Chem 2000;275:35715-35722.
35. Kon K, Ikejima K, Hirose M, Yoshikawa M, Enomoto N, Kitamura T, et al. Pioglitazone prevents early-phase hepatic fibrogenesis caused by carbon tetrachloride. Biochem Biophys Res Commun 2002;291:55-61.
36. Galli A, Crabb DW, Ceni E, Salzano R, Mello T, Svegliati-Baroni G, et al. Antidiabetic thiazolidinediones inhibit collagen synthesis and hepatic stellate cell activation in vivo and in vitro. Gastroenterology 2002;122:1924-1940.
37. Belfort R, Harrison SA, Brown K, Darland C, Finch J, Hardies J, et al. A placebo-controlled trial of pioglitazone in subjects with nonalcoholic steatohepatitis. N Engl J Med 2006;355:2297-2307.
38. Turmelle YP, Shikapwashya O, Tu S, Hruz PW, Yan Q, Rudnick DA. Rosiglitazone inhibits mouse liver regeneration. FASEB J 2006;20:2609-2611.
39. Yamamoto Y, Ono T, Dhar DK, Yamanoi A, Tachibana M, Tanaka T, et al. Role of peroxisome proliferator-activated receptor-gamma (PPAR-gamma) during liver regeneration in rats. J Gastroenterol Hepatol 2008; 23:930-937.

J Gastroenterol (2009) 44:847–855
DOI 10.1007/s00535-009-0073-3

ORIGINAL ARTICLE—LIVER, PANCREAS, AND BILIARY TRACT

# The tumor suppressor protein PTEN inhibits rat hepatic stellate cell activation

**Motoki Takashima · Christopher J. Parsons · Kenichi Ikejima · Sumio Watanabe · Eric S. White · Richard A. Rippe**

Received: 23 February 2009 / Accepted: 5 April 2009 / Published online: 13 May 2009


**Abstract**
*Background* Following a fibrogenic stimulus, the hepatic stellate cell (HSC) transforms from a quiescent to an activated cell type associated with increased proliferation, collagen and smooth muscle α-actin (αSMA) expression. Phosphatase and Tensin Homolog Deleted on Chromosome Ten (PTEN), a tumor suppressor phosphatase, has been shown to play a role in several nonmalignant diseases. Here, we investigated the role of PTEN during HSC activation.
*Methods* Rat HSCs 2 days after isolation were transduced with adenoviruses expressing either the wild-type (WT) or a dominant negative form of PTEN, and culture-associated activation of HSCs, including morphological changes, expression of αSMA and α1(I) collagen, and cell proliferation, were evaluated. Apoptosis of HSCs was detected by measuring activity of caspase 3/7. Phosphorylation status of Akt, $p70^{S6K}$, and Erk was detected by Western blotting.
*Results* Overexpression of WT-PTEN inhibited phenotypic changes were associated with HSC activation, including morphological changes, expression of αSMA and α1(I) collagen, and HSC proliferation, including cyclin D1 expression. WT-PTEN expression also induced apoptosis in HSCs with increased caspase 3/7 activity. Expression of WT-PTEN also caused decreased activation of Akt, $p70^{S6K}$, and Erk signaling pathways.
*Conclusions* Taken together, these findings show that PTEN represents an important negative regulator for transactivation of HSCs. This may have important implications for the design of therapeutic strategies to prevent the progression of liver fibrosis.

**Keywords** Hepatic stellate cells · Phosphatase and Tensin Homolog Deleted on Chromosome Ten (PTEN) · Liver fibrosis · Smooth muscle α-actin (αSMA) · Collagen

M. Takashima · C. J. Parsons · R. A. Rippe (✉)
Division of Gastroenterology and Hepatology,
Department of Medicine,
University of North Carolina, CB #7032,
Medical Biomolecular Research Building,
Room 7340B, Chapel Hill, NC 27599-7032, USA
e-mail: rarippe@med.unc.edu

M. Takashima · K. Ikejima · S. Watanabe
Department of Gastroenterology,
Juntendo University School of Medicine,
Tokyo, Japan

E. S. White
Division of Pulmonary and Critical Care Medicine,
University of Michigan Medical School,
Ann Arbor, Michigan, USA

## Introduction

Liver fibrosis, and its end stage disease liver cirrhosis, represents a major medical problem worldwide. The hepatic stellate cell (HSC) plays a critical role in the development and maintenance of liver fibrosis. In the normal liver, HSCs reside in a quiescent state characterized by vitamin A storage, a low proliferative rate, and trace production of ECM components. However, following a fibrogenic stimulus, HSCs undergo a complex activation process associated with morphological changes from a quiescent vitamin A-storing cell to that of an activated myofibroblast-like cell [1, 2]. HSC activation is also associated with a dramatic increase in the synthesis and deposition of ECM components, of which type I collagen predominates, the appearance of the characteristic activation marker smooth muscle α-actin (αSMA), and an increase in cellular proliferation.

The tumor suppressor protein Phosphatase and Tensin Homolog Deleted on Chromosome Ten (PTEN) is a dual specificity protein and lipid phosphatase [3]. Deletions or mutations of PTEN have been found to occur in a wide range of advanced cancers including glioblastoma, melanoma, endometrial carcinoma, prostate, breast, kidney, and small cell lung cancer [3, 4]. Altered PTEN expression has also been associated with nonmalignant diseases characterized by tissue destruction and remodeling, such as pulmonary fibrosis, bronchial asthma, and rheumatoid arthritis [5–7]. Hepatocyte specific deletion of PTEN showed increased steatosis as well as increased risk for the development of hepatocellular carcinoma [8, 9]. A number of studies have indicated that PTEN is effective at dephosphorylating proteins, and that 3,4,5-trisphosphate ($PIP_3$), a product of phosphatidylinositol-3-kinase (PI3K), is the primary physiologic substrate of PTEN [10, 11]. $PIP_3$ is necessary for phosphorylation and subsequent activation of the downstream target Akt, a kinase that promotes cell survival and growth in various cell types [12–14]. Furthermore, it has been reported that PTEN induces apoptosis, and inhibits proliferation and migration in some normal cell types [15]; however, the fundamental roles of PTEN in normal cells remain largely unknown.

The PI3K-Akt signaling pathway is activated in HSCs by platelet-derived growth factor (PDGF) and promotes cellular proliferation and collagen gene expression [16–18]. Inhibiting PI3K activity suppresses cell proliferation and type I collagen gene expression in activated HSCs [17]. Therefore, the PI3K/Akt signaling pathway represents an important intracellular signaling pathway associated with the fibrogenic nature of HSC activation. The role of PTEN in HSC activation has not been investigated; however, given the role of PTEN in mediating Akt activation, we hypothesized that PTEN plays an important role in regulating cellular functions associated with the development of HSC phenotype. Here, we investigated whether overexpression of PTEN inhibits activation, proliferation, and survival of HSCs.

## Materials and methods

### Hepatic stellate cell isolation

HSCs were purified from Sprague-Dawley rats (>400 g, Charles River Laboratory, Cambridge, MA, USA) by sequential digestion of the liver with pronase and collagenase, followed by Nycodenz gradient centrifugation as previously described [19]. Cell purity, assessed by examining the autofluorescence properties of the stored retinoids in HSCs, was typically between 90 and 95%. HSCs were cultured in Dulbecco's Modified Eagle's Medium (Invitrogen, Carlsbad, CA, USA) supplemented with 10% fetal bovine serum (FBS), and 2 mM L-glutamine, and cultured in a 95% air–5% $CO_2$ humidified atmosphere at 37°C. The growth medium was changed every other day. HSCs were activated by culturing on plastic for 7 days [20]. All animal procedures were performed under the guidelines set by the University of North Carolina Institutional Animal Care and Use Committee and are in accordance with those set by the National Institutes of Health.

### Adenoviral transduction

Ad5-$\beta$gal, which contains the $\beta$-galactosidase gene driven by the cytomegalovirus promoter, was used as a control virus throughout this study. Ad5-wild-type PTEN (Ad5-WT-PTEN) expresses the active form of PTEN, while Ad5-C124S PTEN expresses a dominant negative form of PTEN; both viruses were kindly provided by Dr. C. Kontos (Department of Medicine, Duke University Medical Center, Durham, NC, USA). The C124S mutation results in a phosphatase-dead protein, which possesses neither lipid nor protein phosphatase activity [21]. Viral amplification was performed in 293 cells and the virus purified by cesium chloride centrifugation by standard methodology [22]. HSCs, 2 days after isolation (day 2), were transduced at a multiplicity of infection (MOI) of 150 for 16 h in Dulbecco's Modified Eagle's Medium containing 2% fetal bovine serum (FBS). After 16 h, the transduction medium was changed to fresh growth medium containing 10% FBS. In some of the experiments, HSCs were cultured for 48 h in medium without FBS supplementation to synchronize the cells. Afterwards, cells were treated with 10% FBS. Viral transduction efficiencies were typically between 85 and 95% as assessed by the percentage of GFP-positive cells (data not shown).

### Western blot analysis

Cultured HSCs were washed with phosphate-buffered saline, and the cells were lysed using protein sample buffer (100 mM Tris–HCl, pH 6.8, 200 mM dithiothreitol, 4% SDS, 0.2% bromophenol blue, 20% glycerol). Western blot analysis was performed as described previously [23]. Anti-phospho-Akt ($Ser^{473}$), anti-Akt, anti-phospho-Erk, anti-PTEN or anti-cleaved-caspase 3 (Cell Signaling, Beverly, MA, USA) antibodies were incubated for 16 h at 4°C followed by 1 h incubation at room temperature with horseradish peroxidase-conjugated goat anti-rabbit or goat anti-mouse secondary antibody (Santa Cruz Biotechnology, Santa Cruz, CA, USA), each diluted 1:3000; primary anti-phospho-$p70^{S6K}$, anti-cyclin D1, anti-GAPDH (Santa Cruz Biotechnology, Santa Cruz, CA, USA), anti-$\alpha$SMA, or anti-PCNA antibody (Dako, Carpinteria, CA, USA) incubated

1 h at room temperature followed by 1 h incubation at room temperature with horseradish peroxidase-conjugated goat anti-rabbit or goat anti-mouse secondary antibody each diluted 1:3000. Signals were quantitated by Alpha Imager analysis (Alpha Innotech, San Leandro, CA, USA).

### Cell proliferation studies

Isolated HSCs were seeded at a density of $3 \times 10^5$ cells/plate in 60 mm tissue culture dishes. HSCs were transduced with the adenoviruses on day 2 after cell isolation (average cell number; $1.57 \times 10^5$) as described above. HSCs were counted using a hemocytometer, and cell viability assessed by Trypan blue staining every other day for 10 days.

### RNase protection assay

Total RNA was isolated from rat HSCs cultured for 7 days, and RNase protection assays performed as described previously [24]. Radiolabeled probes were prepared for rat α1(I) collagen [24] and glyceraldehyde-3-phosphate dehydrogenase (pTRI-GAPDH-Rat, Ambion Inc., Austin, TX, USA) then were hybridized with 5 μg of total HSC RNA. Protected fragments were separated using standard 6% acrylamide/urea sequencing gels. Following electrophoresis, bands were visualized by autoradiography and quantitated by PhosphorImager analysis (Amersham Biosciences, Piscataway, NJ, USA).

### Caspase 3/7 Assay

Caspase 3/7 activity was measured using a Caspase 3/7 assay kit (Promega, Madison, WI, USA). HSCs were harvested 48 h after viral transduction and protein extracts prepared following the manufacturers' instructions. Caspase activity was measured in 96-well plate by product absorbance at excitation: 485 nm—emission: 525 nm every 15 min for 16 h at 37°C using a fluorescent microplate reader (Molecular Devices, Sunnyvale, CA, USA).

### Statistical analysis

Results were analyzed for statistical significance according to the Student's $t$ test. Statistical values of $p < 0.05$ were considered to be significant. Data are presented as means ± SEM.

## Results

### Overexpression of PTEN inhibits HSC activation

To investigate endogenous PTEN expression during HSC activation, HSCs were isolated and cultured for 0, 2, and 7 days. PTEN expression was not detected in freshly isolated, quiescent HSCs (day 0); however, after 2 days in culture PTEN expression was weakly detected and was prominent after 7 days in culture (Fig. 1a). Therefore, HSC activation is associated with the induction of PTEN expression.

To determine the effect of PTEN overexpression on morphological changes associated with HSC activation, HSCs were transduced on day 2 with Ad5-WT-PTEN, dominant negative Ad5-C124S PTEN, or Ad5-βgal as a control virus. HSCs transduced with Ad5-βgal and Ad5-C124S and cultured for 7 days appeared to undergo the typical activation process of HSCs when untreated and cultured on plastic (Fig. 1b). The cells showed reduced lipid droplets after 4 and 7 days in culture, and they exhibited enlarged cellular bodies with increased cell numbers. In contrast, HSCs transduced with Ad5-WT-PTEN maintained their star-like processes and cytoplasmic

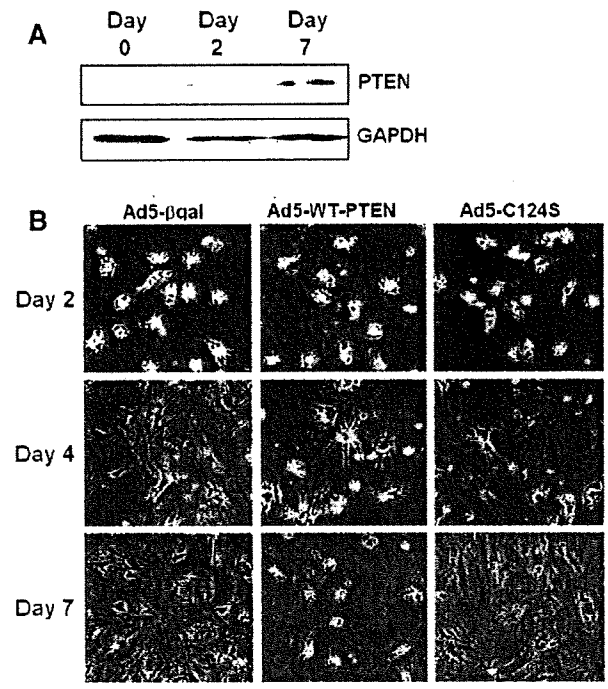


**Fig. 1** Expression of PTEN and morphological changes in HSCs during culture-activation. **a** HSC activation increases endogenous PTEN expression. Cell extracts were prepared from freshly isolated HSCs (day 0) or from cells cultured for 2 or 7 days. PTEN expression was assessed by Western blot analysis. GAPDH was used as an internal control. The data presented is representative of three independent experiments. **b** PTEN overexpression inhibits activation-associated morphological changes. HSCs (day 2 in culture) were transduced with Ad5-βgal, Ad5-WT-PTEN, or Ad5-C124S-PTEN at a MOI of 150. After 16 h, the transduction medium was changed to fresh growth medium and subsequently changed every 48 h. Cell morphology was monitored at days 2, 4, and 7 by phase contrast microscopy (×100)

lipid droplets. In addition, the cells did not appear to proliferate during the 7 day culture period (Fig. 1b). These results demonstrate that overexpression of PTEN in HSCs prevents morphological changes typically associated with activation, including cell spreading and loss of the cytoplasmic lipid droplets, and that its phosphatase activity is responsible for this inhibitory effect.

To investigate the effect of PTEN on αSMA expression, a characteristic biomarker for HSC activation, HSCs were transduced with Ad5-WT-PTEN, Ad5-C124S, or Ad5-βgal. Both Ad5-WT-PTEN and Ad5-C124S viruses were shown to overexpress immunodetectable PTEN (Fig. 2). Ad5-WT-PTEN reduced αSMA expression 66% in HSCs compared to untransduced control cells (Fig. 2). Transduction of HSCs with either Ad5-C124S or Ad5-βgal showed no effect on αSMA expression. Therefore, PTEN expression inhibits the induction of αSMA expression typically associated with HSC activation in HSCs.

The activated HSC is the predominant hepatic cell type in the liver responsible for the increased synthesis and deposition of type I collagen during fibrosis. To assess the role of PTEN on α1(I) collagen mRNA steady state expression, day 2 HSCs were transduced with Ad5-WT-PTEN, Ad5-C124S, or Ad5-βgal and 72 h later α1(I) collagen gene expression assessed. Ad5-WT-PTEN reduced α1(I) collagen mRNA steady state levels by 65%, while Ad5-C124S and Ad5-βgal had no effect on α1(I) collagen expression compared to the control (Fig. 3). These findings indicate that PTEN overexpression is able to decrease α1(I) collagen mRNA expression in HSCs, which is dependent on its phosphatase activity.

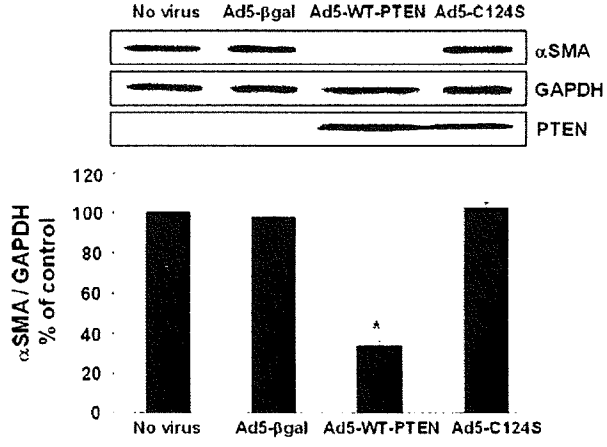


**Fig. 2** PTEN overexpression inhibits αSMA expression in HSCs. HSCs were transduced with Ad5-WT-PTEN, Ad5-C124S, or Ad5-βgal, as a control. Cell extracts were prepared after 48 h following viral transduction and Western blot analysis performed to assess αSMA expression. GAPDH was used as an internal control. Adenoviral expression of WT-PTEN and DN-PTEN (Ad5-C124S) was confirmed by assessing PTEN expression. Graphical analyses from three independent experiments are shown. *Error bars* represent SEM. $*p < 0.05$ versus no virus and Ad5-βgal

## Overexpression of PTEN inhibits proliferation of HSCs with reduced cyclin D1 and PCNA expression

Since the morphological studies suggested that PTEN expression inhibited HSC proliferation during the activation process, we further investigated the mechanism by which PTEN reduces HSC proliferation. HSCs, cultured for 2 days, were either left untreated or transduced with Ad5-WT-PTEN, Ad5-C124S, or Ad5-βgal. HSCs transduced with Ad5-WT-PTEN began to show reduced cell numbers 2 days following WT-PTEN overexpression showing a 24% reduction in cell numbers from the starting number of cells. After days 6 and 10 (4 and 6 days following viral transduction) cell numbers decreased 48 and 70%, respectively. Cells untreated or transduced with Ad5-C124S or Ad-βgal showed increased cell numbers and proliferated at similar rates throughout the 8 day culture period as the untreated cells (Fig. 4a).

To investigate the mechanism by which PTEN inhibited proliferation of HSCs we investigated the effect of PTEN expression on cyclin D1 and PCNA expression. Overexpression of PTEN reduced cyclin D1 expression by 96% and PCNA expression by 93%, compared to untreated control cells while transduction with either Ad5-C124S or Ad5-βgal had no effect on the expression of either cyclin D1 or PCNA (Fig. 4b). Together, these results indicate that PTEN expression inhibits cellular proliferation which is associated with reduced expression of both cyclin D1 and PCNA in HSCs.

## PTEN expression induced apoptosis in HSCs

Our results suggest that PTEN expression may actually promote cell death in HSCs. To further investigate this possibility we examined the potential role of apoptosis by examining cleavage of caspase 3, a marker of apoptosis, in HSCs overexpressing PTEN. Transduction of HSCs with Ad5-WT-PTEN induced caspase 3 cleavage, whereas cells transduced with either Ad5-βgal or Ad5-C124S did not result in caspase 3 cleavage (Fig. 5a). To quantitate this apoptotic effect, we measured caspase 3/7 activity. PTEN overexpression increased caspase 3/7 activity 4.4-fold compared to the control cells (Fig. 5b). However, transduction of HSCs with either Ad5-C124S or Ad5-βgal showed no significant increase in caspase 3/7 activity (Fig. 5b). These findings show that PTEN overexpression in HSCs blocks HSC proliferation, which is mediated by reduced cyclin D1 and PCNA expression, and also induces apoptosis, which is associated with increased caspase3/7 activity.

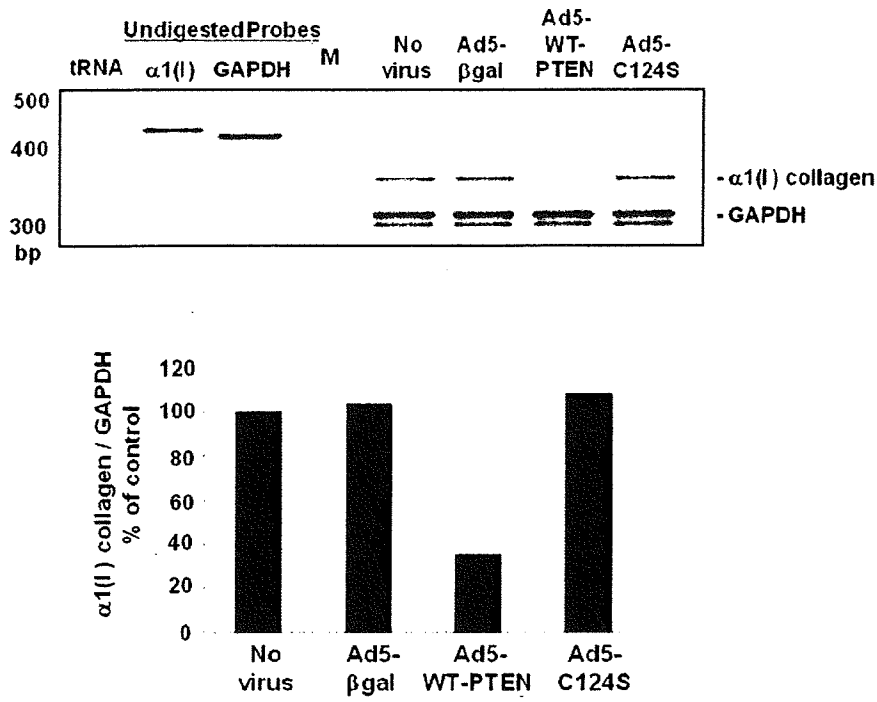


**Fig. 3** PTEN overexpression suppresses α1(I) collagen mRNA expression in HSCs. Day 2 HSCs were transduced with Ad5-WT-PTEN, Ad5-C124S, or Ad5-βgal. Cells were serum-starved for 48 h then stimulated with 10% serum for 24 h, before total RNA was isolated at day 7. Total RNA, 5 μg, was hybridized with radiolabeled probes for either α1(I) collagen or GAPDH, used as an internal control. tRNA was used as a negative control RNA sample; *M* 100 bp ladder. Graphical analysis is representative of three individual RNase protection assays. Expression of α1(I) collagen mRNA was normalized to GAPDH levels. *Error bars* represent SEM. $^{*}p < 0.05$ versus no virus and Ad5-βgal

Increased PTEN expression inhibits serum-induced phosphorylation of Akt, $p70^{S6K}$, and Erk in HSCs

Akt is a downstream target of PI3K and an important cell survival factor in various cell types, particularly cancer cells [25]. We have previously shown that serum and PDGF both stimulate Akt phosphorylation at $Ser^{473}$ in HSCs [17]. We used serum stimulation to assess the role of PTEN on Akt phosphorylation. HSCs transduced with the control adenovirus, Ad5-βgal, showed increased $Ser^{473}$ phosphorylation of Akt following serum stimulation which peaked at 30 min that gradually decreased over the 120 min time period. However, serum-induced Akt phosphorylation was nearly completely blocked in HSCs transduced with Ad5-WT-PTEN (Fig. 6a).

As a downstream target of Akt, $p70^{S6K}$ has been shown to regulate proliferation and cell survival in several cell types including HSCs [16, 26–28]. To investigate the effect of PTEN on $p70^{S6K}$ activation by assessing its phosphorylation status, quiescent HSCs were transduced with Ad5-WT-PTEN or Ad5-βgal. In control HSCs, $p70^{S6K}$ phosphorylation was induced and reached maximal levels within 30 min after serum treatment which remained elevated for at least 120 min (Fig. 6b). In contrast, transduction of HSCs with Ad5-WT-PTEN completely blocked phosphorylation of $p70^{S6K}$ at all time points. Extracellular signal-regulated kinase (ERK) is a member of the mitogen-activated protein kinase (MAPK) family. In HSCs, PDGF-induced ERK activation is a result of the sequential activation of Ras-Raf-MEK signaling [29]. In addition, inhibition of ERK phosphorylation has been shown to block HSC proliferation [30]. To investigate the role of PTEN on ERK phosphorylation, HSCs were transduced with Ad5-WT-PTEN, Ad5-C124S, or Ad5-βgal, and the effects on ERK phosphorylation assessed following serum stimulation. Following serum treatment, HSCs transduced with Ad5-βgal exhibited a transient increase in ERK phosphorylation which reached peaked after 30 min and was diminished after 120 min. However, transduction with Ad5-WT-PTEN efficiently blocked serum-induced ERK phosphorylation at all time points assessed (Fig. 6c).

## Discussion

Activation of PI3K signaling is an important event during HSC activation where we and others have shown it regulates cell proliferation and collagen gene expression, two critical aspects for activated HSCs in the fibrogenic process [17, 31]. In this study, we investigated the potential of PTEN to negatively regulate PI3K activity and prevent the activation of HSCs into fibrogenic cells. Here, we showed that PTEN has a significant role in regulating HSC activation. HSCs, when cultured on plastic become activated, which is associated with a loss of their stored retinoids, they express type I collagen and αSMA, and the cells proliferate. When day 2 cultured HSCs were transduced with WT-PTEN, the cells failed to activate. This was

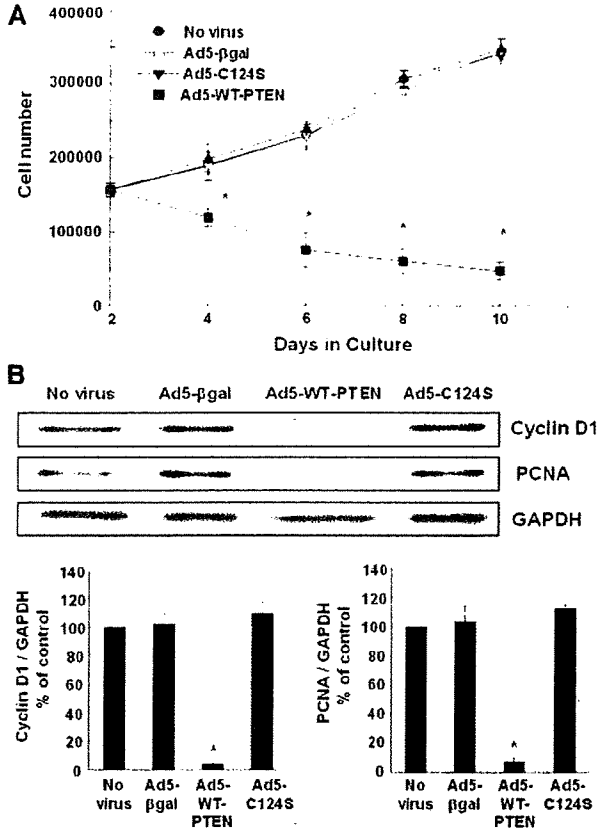


**Fig. 4** PTEN overexpression inhibits HSC proliferation. **a** Overexpression of PTEN inhibits HSC proliferation. Day 2 HSCs were transduced with Ad5-WT-PTEN, Ad5-C124S, or Ad5-$\beta$gal and cell numbers assessed by manual cell counts using a hemocytometer every 48 h until day 10. Results are representative of three independent experiments. *Error bars* represent SEM. $*p < 0.05$ versus no virus and Ad5-$\beta$gal. **b** PTEN inhibits expression of cyclin D1 and PCNA in HSCs. Day 2 HSCs were transduced with Ad5-WT-PTEN, Ad5-C124S, or Ad5-$\beta$gal. Cell extracts were prepared 48 h following viral transduction and Western blot analysis performed for cyclin D1 or PCNA expression. GAPDH was used as an internal control. Graphical analyses from three separate experiments are shown. *Error bars* represent SEM. $*p < 0.05$ versus no virus and Ad5-$\beta$gal

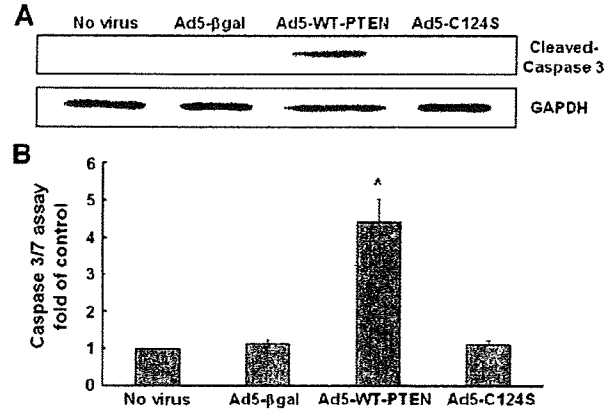


**Fig. 5** PTEN overexpression induces apoptosis in HSCs. **a** Day 2 HSCs were transduced with Ad5-WT-PTEN, Ad5-C124S, or Ad5-$\beta$gal. Total cell extracts (20 $\mu$g) were prepared 48 h after viral transduction and Western blot analysis performed using a cleaved-caspase3 antibody. GAPDH was used as an internal control. **b** Caspase3/7 activities were measured in control and Ad5-WT-PTEN, Ad5-C124S, or Ad5-$\beta$gal transduced HSCs. Product absorbance was read at excitation: 485 nm/emission: 525 nm every 15 min for 16 h at 37°C using a fluorescent microplate reader. Data are representative of three independent studies. *Error bars* represent SEM. $*p < 0.05$; versus no virus and Ad5-$\beta$gal

associated with the cells remaining small in size, retaining their stored retinoids (Fig. 1b), even after 7 days in culture, and the cells failing to proliferate (Figs. 1b, 4a). In addition, overexpression of PTEN inhibited the induction of both αSMA and α1(I) collagen gene expression, both markers of activated HSCs (Fig. 2). In contrast, day 2 HSCs transduced with Ad5-$\beta$gal or Ad5-C124S, a dominant negative PTEN which lacks lipid and protein phosphatase activity, activated in a normal manner where they lost their stored retinoid droplets within 4 days in culture, and by day 7 they exhibited enlarged cell bodies and transformed into myofibroblast-like cells associated with the expression of αSMA and α1(I) collagen, classical markers for activated HSCs. These observations are consistent with the previous reports, in terms of down-regulation of α1(I) collagen gene expression through inhibition of the PI3K-Akt pathway [16–18]. On the other hand, the role of PTEN in αSMA expression has not been fully clarified. Our findings suggested that PTEN also plays a regulatory role on expression of αSMA upon transactivation of HSCs.

PTEN is a negative regulator of PI3K signaling. PI3K activity phosphorylates $PIP_2$ to generate $PIP_3$. $PIP_3$ binds to the plekstrin homology domain of Akt, directing it to the cell membrane where it becomes activated by phosphorylation events to initiate cell survival mechanisms. Thus, Akt represents a downstream target of PI3K, mediating cell survival by phosphorylating and inactivating several proapoptotic targets, including Bad, GSK-3$\beta$, and forkhead family proteins [31]. We have previously shown that $p70^{S6K}$, a downstream target of Akt, plays an important role in PDGF-induced HSC proliferation and cell cycle control [16]. Overexpression of a constitutively active form of Akt stimulates $p70^{S6K}$ and promotes cell proliferation and cell survival [26–28]. PI3K/Akt signaling is activated in HSCs following PDGF or serum stimulation of HSCs [18]. A role for PI3K in HSC proliferation was supported in an in vivo study in rats which demonstrated that $CCl_4$ treatment leads to autophosphorylation of the PDGF receptor and increased PI3K activity [18]. Activation of PI3K is also important for HSC proliferation and chemotaxis in activated HSCs [18]. Furthermore, blocking PI3K with the chemical inhibitor LY294002 inhibits HSC

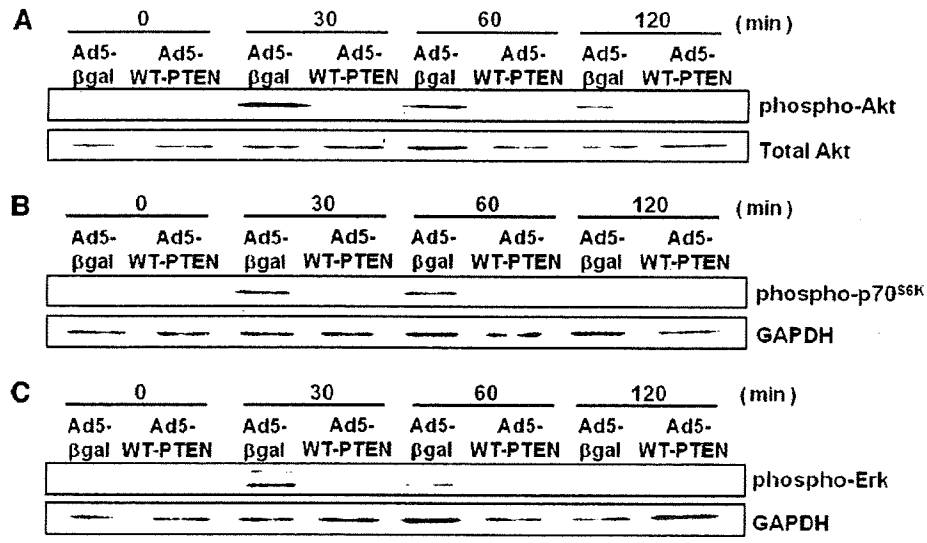


**Fig. 6** PTEN inhibits serum-induced phosphorylation of Akt, $p70^{S6K}$, and Erk in HSCs. HSCs were transduced with Ad5-WT-PTEN or Ad5-$\beta$gal on day 2, then serum starved for 48 h. Cellular proteins were harvested 0, 30, 60, and 120 min following stimulation with 10% serum. Western blot analysis was performed using anti-phospho-Akt ($Ser^{473}$) (**a**), anti-phospho-$p70^{S6K}$(**b**), or anti-phospho-Erk (**c**). GAPDH and total Akt were examined as internal controls. Results are representative of three independent experiments

proliferation [17, 32]. PDGF also activates ERK in HSCs by sequential activation of Ras-Raf-MEK signaling [29]. A role of ERK in HSC proliferation was shown when inhibition of ERK phosphorylation blocked cell proliferation in activated HSCs [30].

The molecular mechanism of PTEN's effect on PI3K-Akt-$p70^{S6K}$ and Erk signaling pathways has not been clarified in HSCs. Here we showed that overexpression of PTEN blocked serum-induced phosphorylation of Akt, $p70^{S6K}$, and Erk in HSCs (Fig. 6). These findings suggest that both PI3K-Akt and Erk signaling pathways are targets of PTEN in HSCs. $p70^{S6K}$ is required for G1 cell-cycle progression and cell growth [33]. It phosphorylates the S6 protein of the 40S ribosomal subunit and is involved in translational control of 5′-oligopyrimidine tract mRNAs [33, 34]. Rapamycin, an inhibitor of mTOR and thus the downstream kinase $p70^{S6K,}$ blocks protein synthesis and inhibits cell cycle progression at the G1/S transition [35]. Previous studies have shown that D-type cyclins play an important role in cell cycle progression, and that expression of cyclin D1, D2, and E correlates with cellular proliferation [36, 37]. Furthermore, cyclin D expression is post-transcriptionally regulated via the PI3K/Akt pathway [38], and inhibition of PI3K is able to block cyclin D1 expression in rat HSCs [39]. We assessed the role of PTEN on HSC proliferation and showed that increased PTEN expression dramatically reduces expression of cyclin D1 and PCNA in HSCs (Fig. 4b). This may potentially be a result of PTEN inhibition of $p70^{S6K}$ phosphorylation and may explain the mechanism by which PTEN inhibits proliferation of HSCs.

We also observed that PTEN reduced cell numbers when overexpressed in HSCs (Fig. 4a). This was likely mediated in part by an increase in apoptosis since the number of Ad5-WT-PTEN-transduced HSCs was significantly lower than that of control cells. In addition, overexpressing PTEN induced cleavage of the proapoptotic caspase 3 and induced caspase3/7 activity. PTEN is not expressed in quiescent HSCs, but it does become induced following HSC activation (Fig. 1a). We showed that when PTEN overexpressed early during the activation process, the cells fail to activate and undergo apoptosis-mediated cell death. Since PTEN is a negative regulator of PI3K signaling, our results indicate that PI3K signaling is pivotal for the development of the activated state in HSCs, as overexpressing PTEN during the early stages of activation induced apoptotic-mediated cell death. We believe that PI3K signaling provides cell survival signals during HSC activation, probably mediated through cell survival signals via Akt activation as well as proliferative signaling mediated by $p70^{S6K}$ signaling. Together, these findings have important ramifications for the design of therapeutic strategies to treat liver fibrosis.

Regarding the therapeutic implication, experimental approaches using overexpression of PTEN have been evaluated in other types of cells; for instance, it has been reported that overexpression of PTEN using adenovirus inhibits the growth of human prostate cancer xenografts in mice through induction of apoptosis and inhibition of angiogenesis and cellular proliferation [40]. In addition, adenoviral overexpression of PTEN has been demonstrated to reduce the symptoms of asthma by inhibiting VEGF expression in mice [41]. The gene manipulation of PTEN, however, needs attention since there might be serious adverse effects relating to development, tissue repair, and metabolism, especially in case targeting is insufficient [42–44]. To establish the PTEN-directed gene therapy for hepatic fibrosis, development of cell-specific gene

modulation for HSCs is essential. In conclusion, our results would suggest that inducing PTEN expression during fibrosis would limit the progression of fibrosis and may potentially promote the resolution of liver fibrosis.

**Acknowledgment** This work was partially funded by: NIH-DK065972 (R.A.R.) and NIH-HL070990 (E.S.W.).

## References


1. Friedman SL. Molecular regulation of hepatic fibrosis, an integrated cellular response to tissue injury. J Biol Chem. 2000;275:2247–50.
2. Eng FJ, Friedman SL, Fibrogenesis I. New insights into hepatic stellate cell activation: the simple becomes complex. Am J Physiol Gastrointest Liver Physiol. 2000;279:G7–11.
3. Li J, Yen C, Liaw D, Podsypanina K, Bose S, Wang SI, et al. PTEN, a putative protein tyrosine phosphatase gene mutated in human brain, breast, and prostate cancer. Science. 1997; 275:1943–7.
4. Steck PA, Pershouse MA, Jasser SA, Yung WK, Lin H, Ligon AH, et al. Identification of a candidate tumour suppressor gene, MMAC1, at chromosome 10q23.3 that is mutated in multiple advanced cancers. Nat Genet. 1997;15:356–62.
5. Kwak YG, Song CH, Yi HK, Hwang PH, Kim JS, Lee KS, et al. Involvement of PTEN in airway hyperresponsiveness and inflammation in bronchial asthma. J Clin Invest. 2003;111:1083–92.
6. White ES, Thannickal VJ, Carskadon SL, Dickie EG, Livant DL, Markwart S, et al. Integrin alpha4beta1 regulates migration across basement membranes by lung fibroblasts: a role for phosphatase and tensin homologue deleted on chromosome 10. Am J Respir Crit Care Med. 2003;168:436–42.
7. Pap T, Franz JK, Hummel KM, Jeisy E, Gay R, Gay S. Activation of synovial fibroblasts in rheumatoid arthritis: lack of expression of the tumour suppressor PTEN at sites of invasive growth and destruction. Arthritis Res. 2000;2:59–64.
8. Horie Y, Suzuki A, Kataoka E, Sasaki T, Hamada K, Sasaki J, et al. Hepatocyte-specific PTEN deficiency results in steatohepatitis and hepatocellular carcinomas. J Clin Invest. 2004;113:1774–83.
9. Sato W, Horie Y, Kataoka E, Ohshima S, Dohmen T, Iizuka M, et al. Hepatic gene expression in hepatocyte-specific Pten deficient mice showing steatohepatitis without ethanol challenge. Hepatol Res. 2006;34:256–65.
10. Maehama T, Dixon JE. The tumor suppressor, PTEN/MMAC1, dephosphorylates the lipid second messenger, phosphatidylinositol 3, 4, 5-trisphosphate. J Biol Chem. 1998;273:13375–8.
11. Li L, Ernsting BR, Wishart MJ, Lohse DL, Dixon JE. A family of putative tumor suppressors is structurally and functionally conserved in humans and yeast. J Biol Chem. 1997;272:29403–6.
12. Datta SR, Brunet A, Greenberg ME. Cellular survival: a play in three Akts. Genes Dev. 1999;13:2905–27.
13. Testa JR, Bellacosa A. AKT plays a central role in tumorigenesis. Proc Natl Acad Sci USA. 2001;98:10983–5.
14. Testa JR, Tsichlis PN. AKT signaling in normal and malignant cells. Oncogene. 2005;24:7391–3.
15. White ES, Atrasz RG, Hu B, Phan SH, Stambolic V, Mak TW, et al. Negative regulation of myofibroblast differentiation by PTEN (Phosphatase and Tensin Homolog Deleted on chromosome 10). Am J Respir Crit Care Med. 2006;173:112–21.
16. Gabele E, Reif S, Tsukada S, Bataller R, Yata Y, Morris T, et al. The role of p70S6K in hepatic stellate cell collagen gene expression and cell proliferation. J Biol Chem. 2005;280:13374–82.
17. Reif S, Lang A, Lindquist JN, Yata Y, Gabele E, Scanga A, et al. The role of focal adhesion kinase-phosphatidylinositol 3-kinase-Akt signaling in hepatic stellate cell proliferation and type I collagen expression. J Biol Chem. 2003;278:8083–90.
18. Marra F, Gentilini A, Pinzani M, Choudhury GG, Parola M, Herbst H, et al. Phosphatidylinositol 3-kinase is required for platelet-derived growth factor's actions on hepatic stellate cells. Gastroenterology. 1997;112:1297–306.
19. Weiskirchen R, Gressner AM. Isolation and culture of hepatic stellate cells. Methods Mol Med. 2005;117:99–113.
20. Rockey DC, Boyles JK, Gabbiani G, Friedman SL. Rat hepatic lipocytes express smooth muscle actin upon activation in vivo and in culture. J Submicrosc Cytol Pathol. 1992;24:193–203.
21. Myers MP, Pass I, Batty IH, Van der Kaay J, Stolarov JP, Hemmings BA, et al. The lipid phosphatase activity of PTEN is critical for its tumor suppressor function. Proc Natl Acad Sci USA. 1998;95:13513–8.
22. Xing Z, Ohkawara Y, Jordana M, Graham F, Gauldie J. Transfer of granulocyte-macrophage colony-stimulating factor gene to rat lung induces eosinophilia, monocytosis, and fibrotic reactions. J Clin Invest. 1996;97:1102–10.
23. Tsukada S, Westwick JK, Ikejima K, Sato N, Rippe RA. SMAD and p38 MAPK signaling pathways independently regulate alpha1(I) collagen gene expression in unstimulated and transforming growth factor-beta-stimulated hepatic stellate cells. J Biol Chem. 2005;280:10055–64.
24. Rippe RA, Almounajed G, Brenner DA. Sp1 binding. activity increases in activated Ito cells. Hepatology. 1995;22:241–51.
25. Sen P, Mukherjee S, Ray D, Raha S. Involvement of the Akt/PKB signaling pathway with disease processes. Mol Cell Biochem. 2003;253:241–6.
26. Kim AH, Khursigara G, Sun X, Franke TF, Chao MV. Akt phosphorylates and negatively regulates apoptosis signal-regulating kinase 1. Mol Cell Biol. 2001;21:893–901.
27. Kulik G, Klippel A, Weber MJ. Antiapoptotic signalling by the insulin-like growth factor I receptor, phosphatidylinositol 3-kinase, and Akt. Mol Cell Biol. 1997;17:1595–606.
28. Coffer PJ, Jin J, Woodgett JR. Protein kinase B (c-Akt): a multifunctional mediator of phosphatidylinositol 3-kinase activation. Biochem J. 1998;335(Pt 1):1–13.
29. Pinzani M, Marra F. Cytokine receptors and signaling in hepatic stellate cells. Semin Liver Dis. 2001;21:397–416.
30. Marra F, Arrighi MC, Fazi M, Caligiuri A, Pinzani M, Romanelli RG, et al. Extracellular signal-regulated kinase activation differentially regulates platelet-derived growth factor's actions in hepatic stellate cells, and is induced by in vivo liver injury in the rat. Hepatology. 1999;30:951–8.
31. Parsons CJ, Takashima M, Rippe RA. Molecular mechanisms of hepatic fibrogenesis. J Gastroenterol Hepatol. 2007;22(Suppl 1):S79–84.
32. Marra F, Pinzani M, DeFranco R, Laffi G, Gentilini P. Involvement of phosphatidylinositol 3-kinase in the activation of extracellular signal-regulated kinase by PDGF in hepatic stellate cells. FEBS Lett. 1995;376:141–5.
33. Pullen N, Thomas G. The modular phosphorylation and activation of p70S6K. FEBS Lett. 1997;410:78–82.
34. Berven LA, Crouch MF. Cellular function of p70S6K: a role in regulating cell motility. Immunol Cell Biol. 2000;78:447–51.
35. Dennis PB, Fumagalli S, Thomas G. Target of rapamycin (TOR): balancing the opposing forces of protein synthesis and degradation. Curr Opin Genet Dev. 1999;9:49–54.
36. Sherr CJ. Cancer cell cycles. Science. 1996;274:1672–7.
37. Stillman B. Cell cycle control of DNA replication. Science. 1996;274:1659–64.
38. Muise-Helmericks RC, Grimes HL, Bellacosa A, Malstrom SE, Tsichlis PN, Rosen N. Cyclin D expression is controlled post-transcriptionally via a phosphatidylinositol 3-kinase/Akt-dependent pathway. J Biol Chem. 1998;273:29864–72.